Storage, patterns and influencing factors for soil organic carbon in coastal wetlands of China

Running title: Controls on SOC stocks in coastal wetlands

Shaopan Xia[1,2], Zhaoliang Song[2,3]*, Lukas Van Zwieten[4], Laodong Guo[5], Changxun Yu[6], Weiqi Wang[7], Qiang Li[2], Iain P. Hartley[8], Yuanhe Yang[9], Hongyan Liu[10], Yidong Wang[11], Xiangbin Ran[12], Congqiang Liu[2,3], Hailong Wang[13,14]

1 Institute of Resource, Ecosystem and Environment of Agriculture, College of Resources and Environmental Sciences, Nanjing Agricultural University, Nanjing 210095, China

2 School of Earth System Science, Institute of Surface-Earth System Science, Tianjin Key Laboratory of Earth Critical Zone Science and Sustainable Development in Bohai Rim, Tianjin University, Tianjin 300072, China

3 Haihe Laboratory of Sustainable Chemical Transformations, Tianjin 300192, China

4 Wollongbar Primary Industries Institute, NSW Department of Primary Industries, Australia

5 School of Freshwater Sciences, University of Wisconsin-Milwaukee, Milwaukee, WI 53204, USA

6 Department of Biology and Environmental Science, Linnaeus University, 39231 Kalmar, Sweden

7 Key Laboratory of Humid Subtropical Eco-Geographical Process, Ministry of Education, Fujian Normal University, Fuzhou, China

8 Geography, College of Life and Environmental Sciences, University of Exeter, Rennes Drive, Exeter EX4 4RJ, UK

9 State Key Laboratory of Vegetation and Environmental Change, Institute of Botany, Chinese Academy of Sciences, 100093 Beijing, China

10 College of Urban and Environmental Sciences, Peking University, Peking 100871, China

11 Tianjin Key Laboratory of Water Resources and Environment, Tianjin Normal University, Tianjin 300387, China

12 First Institute of Oceanography, Ministry of Natural Resources, No. 6 Xianxialing Road, Qingdao 266061, China

13 School of Environment and Chemical Engineering, Foshan University, Foshan, Guangdong, 528000, China

14 School of Environmental and Resource Sciences, Zhejiang A&F University, Hangzhou, Zhejiang, 311300, China

*Correspondence: zhaoliang.song@tju.edu.cn Telephone: +086-15202264081

Address: School of Earth System Science, Tianjin University, Tianjin 300072, China

Abstract: Soil organic carbon (SOC) in coastal wetlands, also known as 'blue C', is an essential component of the global C cycles. To gain a detailed insight into blue C storage and controlling factors, we studied 142 sites across ca. 5000 km of coastal wetlands, covering temperate, subtropical and tropical climates in China. The wetlands represented 6 vegetation types (*Phragmites australis*, mixed of *P. australis* and *Suaeda*, single *Suaeda*, *Spartina alterniflora*, mangrove (*Kandelia obovata* and *Avicennia marina*), tidal flat) and 3 vegetation types invaded by *S. alterniflora* (*P. australis*, *K. obovata*, *A. marina*). Our results revealed large spatial heterogeneity in SOC density of the top 1-meter ranging 40–200 Mg C ha^{-1}, with higher values in mid-latitude regions (25–30º N) compared to those in both low- (20º N) and high- latitude (38–40º N) regions. Vegetation type influenced SOC density, with *P. australis and S. alterniflora* having the largest SOC density, followed by mangrove, mixed *P. australis* and *Suaeda*, single *Suaeda* and tidal flat. SOC density increased by 6.25 Mg ha^{-1} following *S. alterniflora* invasion into *P. australis* community, but decreased by 28.56 and 8.17 Mg ha^{-1} following invasion into *K. obovata* and *A. marina* communities. Based on field measurements and published literature, we calculated a total inventory of 57 $\times 10^6$ Mg C in the top 1-meter soil across China's coastal wetlands. Edaphic variables controlled SOC content, with soil chemical properties explaining the largest variance in SOC content. Climate did not control SOC content, but had a strong interactive effect with edaphic variables. Plant biomass and quality traits were a minor contributor in regulating SOC content, highlighting the importance of quantity and quality of OC inputs and the balance between production and degradation within the coastal wetlands. These findings provide new insights into blue C stabilization mechanisms and sequestration capacity in coastal wetlands.

Keywords: Blue carbon, salt marsh, mangrove, vegetation type, plant invasion, coastal wetlands, climate change

1 Introduction

Global wetlands, represent 6–8% of the world's land surface area, and store approximately 20–30% of the terrestrial soil carbon (C) pool (estimated to contain 2500 Pg C) (Lal, 2008; Nahlik and Fennessy, 2016). Specifically, coastal wetlands which occupy only <0.3% of the ocean surface contribute approximately 47% of the total organic carbon (OC) buried in marine sediments, with an estimated OC accumulation rate of 0.07–0.22 Pg C year^{-1} globally (Hopkinson et al., 2012; Duarte et al., 2013). Coastal wetlands are characterized by high primary productivity, deposition rate, C burial rate and low methane (CH_4) emissions, and thus play an important role in land-ocean ecosystem structure and function (Serrano et al., 2019). Therefore, enhancing the capacity of wetlands to sequester OC is an important component of the global effort to mitigate CO_2 entering the atmosphere contributing to climate change.

Although wetlands function as important C sinks, coastal wetlands are less studied than those of uplands (i.e., cropland, grassland, and forest) due to the challenges posed by hydrological conditions (i.e., Yang et al., 2007; Xu et al., 2018). Thus, it is important to study C stocks at different spatial scales to allow the assessment of C sequestration and fixation. Given the complexity in the biogeochemistry and ecology of coastal wetlands, there is high variability in the quantity and rate of OC buried in underlying soils, depending on geographic settings, vegetation composition, exotic plant invasion and wetland type (e.g., saltmarsh, estuary) across the coastal wetlands (Atwood et al., 2017; Hayes et al., 2017; Osland et al., 2018; Rovai et al., 2018; Xia et al., 2021b). However, most studies on coastal wetland C stocks and sequestration mechanisms have been focused on sites characterized by high C density (Whitaker et al., 2015), a single vegetation type (Gao et al., 2019) or single wetland type (Yan et al., 2008), and sites strongly disturbed by human activities (Kirwan and Megonigal, 2013), or wetlands with *Spartina alterniflora* invasion (Gao et al., 2020). On the other hand, studies focused on a national scale are based on comprehensive meta-analysis using a dataset compiled from published literature rather than field measurements (Xiao et al., 2019). In addition, how different are the SOC density in coastal wetlands with inland wetlands, is not fully clear. Such comparison would strengthen researchers' cognition of the contribution of coastal wetland C storage. Although these existing works are key to understanding the role of coastal wetland C cycles, it is still difficult to accurately quantify the C stocks and processes controlling these stocks due to the paucity in field data to validate models (i.e., soil physico-chemical properties, climate, and vegetation biomass). In addition, data variability among sites likely resulted from differences in methods/protocols and the limited number of sampling locations (Meng et al., 2019; Hinson et al., 2017). The deficiency and regional bias of studies from China's coastal wetlands have limited the reliable estimation of their capability as regional and global C sinks (e.g., Jiao et al., 2018; Liu et al., 2014; Fu et al., 2021). Therefore, it is necessary to measure these variabilities in climate, vegetation and soil conditions to quantify soil organic carbon (SOC) stocks and their uncertainties in coastal wetlands across local and global scales.

To better contribute to achieving carbon neutralization, understanding how the soil C pools and their specific stability in coastal wetlands respond to environmental conditions are important for climate change mitigation and sustainable wetland management (Davidson and Janssens, 2006; Lal, 2004; Han et al., 2020). The predominant factors driving SOC dynamics include climate, plant biological traits, and soil properties (Dungait et al., 2012; Lehmann and Kleber, 2015; Luo et al., 2017). Firstly, climatic variables such as precipitation and temperature are usually considered to be critical (Carvalhais et al., 2014) because of their direct effect on organic C inputs via plant CO_2 assimilation, and output via microbial aerobic and anaerobic respiration. However, the effects of precipitation and temperature on net OC accumulation are highly variable (e.g., Chen et al., 2013; Wang et al., 2020; Luo et al., 2020) with different responses in topsoil and subsoil (Hicks Pries et al., 2017; Melillo et al., 2017; Zhou et al., 2018), including increase, decrease and no change. For example, coastal peat swamp systems are usually C sinks with higher primary productivity and lower CO_2 release because long-term water supersaturation and low temperature in the systems are not favorable for microbial activities and subsequent SOC mineralization (Bernal and Mitsch 2012; Friborg et al., 2003).

Secondly, plant C input is the determinant factor of soil C stocks although higher biomass production may not necessarily result in higher litter C input (Gao et al., 2019). In addition to biomass or litter quantity, litter quality is another important factor regulating organic C stability and preservation (Osland et al., 2018; Bahadori et al., 2021). The vegetation diversity, including native grasses *Phragmites australis*, *Suaeda*, *Acorus calamus*, invasive grasses *Spartina* *alterniflora*, and mangrove *Kandelia obovata*, *Avicennia marina*, *Ceriops tagal*, *Bruguiera sexangular*, can also regulate the quality of C inputs into wetland soils (Yang et al., 2019; Xia et al., 2021a; Fu et al., 2021). The influence of vegetation communities and in particular changes in vegetation composition (i.e., native vs. invasive species or grasses vs. mangrove) on SOC remains relatively unstudied in these wetland systems.

Thirdly, although climatic and biological factors (e.g., plant C inputs) could regulate the magnitude or rate of apparent SOC shifting from one status to another, the final SOC stock capacity of soil is generally controlled by the physicochemical properties of soil (Luo and Raphael, 2020). Increasing evidence has shown that soil geochemistry and physical structure provides a physicochemical barrier to microbial accessibility of SOC (Sun et al., 2019, Duan et al., 2020). The physicochemical environment also regulates the supply of water, oxygen, nutrients, and other resources, which are necessary for microbial communities to utilize SOC, as well as for plant C assimilation and deposition as detritus or rhizodeposits (Luo and Raphael, 2020). The stabilization of organic carbon in soil has been shown to vary significantly because of physical stabilization mechanism, chemical stabilization mechanism, and biochemical protection mechanism (Feng et al., 2013; Sui et al., 2021). However, large field datasets showing spatial heterogeneity of edaphic variables in coastal wetlands remain scarce, which perpetuates the extensive uncertainties about the patterns of SOC stocks and the main controlling factors. It is thus critical to understand the extent to which soil properties and processes regulate SOC stabilization and stocks in different field scenes.

The climatic, biotic, and edaphic factors often interact with each other and collectively regulate SOC dynamics through different processes and mechanisms (Zhang et al., 2002; Yang et al., 2019). However, most previous studies have focused on a single independent factor, with few quantitatively analyzing the relative effects on SOC stocks based on large scale field data. Studies focusing on the effects of a single factor on SOC dynamics may lead to uncertainties in the outcomes (Meng et al., 2019; Tangen et al., 2020). In addition to topsoil layers (e.g., 0–30 cm), deeper soil layers (below 30 cm) could store more organic C than the topsoil layers (Meng et al., 2019). This motivated us to extend our soil sampling to 100 cm to better understand the deep soil C stocks. Such information can provide new insights into mechanisms underpinning

SOC dynamics, which are essential for predicting SOC stocks as well as understanding feedback loops from global environmental change (Belyea et al., 2004).

In the present study, we attempted to sample wetlands across broad regions that include almost all coastal wetlands of China, covering temperate, subtropical and tropical climate zones. Our objectives were to: (1) systematically quantify the SOC content and density in China's coastal wetlands and their interrelationship with the location of wetlands, vegetation type, invasion species, and climatic zone; (2) estimate the total inventory of SOC sequestration and regional variability across China's coastal wetlands and compare SOC density with inland wetlands; (3) explore climatic, biological, and edaphic drivers of the distribution and dynamics of SOC contents and stocks. We hypothesized that (1) SOC contents and densities were largely affected by vegetation type, invasion species, and climatic factors; (2) SOC densities greatly varied among different coastal wetlands and were lower than that of inland wetlands; and (3) SOC dynamics were interactively controlled by climate, plant biological traits and edaphic variables, and the effects of edaphic variables override climate and plant inputs on SOC stocks. This study provides crucial information for understanding the contribution of coastal wetlands in China to the global C cycles, and will allow for the optimization of wetland management strategies and policy decisions at the national scale.

2 Materials and methods

2.1 Study areas

We selected 142 representative wetland sampling sites along China's coast line from Liaoning to Hainan Province (108°–122°E, 20°–40°N) covering temperate, subtropical and tropical climate zones (Figure 1). The sampled wetlands include Liao River Delta (LRD), Duliujian River (DLJR), Nandagang wetland (NDG), Yellow River Estuary (YRE), Linhong River Estuary (LRE), Sheyang River Estuary (SRE), Doulong Harbor (DH), Dafeng Wetland (DW), Qidong Wetland (QW), Wanggang wetland (WGW), Yancheng Wetland (YCW), Chongming Island (CI), Hengsha Island (HI), Yueqing Bay (YB), Minjiang River Estuary (MRE), Jiulong River Estuary (JRE), Zhangjiang River Estuary (ZRE), Zhanjing (ZJ), Beihai (BH), Dongzhai Bay (DB), Qinglan Harbor (QH), Xinying Harbor (XH), Sanya Bay (SYB), Sibi Bay (SBB), Xinyang Bay (XB), Tielu Harbor (TH), Danzhou (DZ) and Lingao (LG) (Table 1). The mean annual precipitation (MAP) and mean annual temperature (MAT) ranged from 551.6 to 1871 mm and from 8.40 to 23.4ºC, respectively. The dominant native species at these sites include *Phragmites australis*, *Suaeda glauca*, *Suaeda salsa*, *Spartina alterniflora*, *Kandelia obovata*, *Avicennia marina*, *Aeluropus littoralis*, *Sonneratia apetala*, *Rhizophora stylosa*, *Aegiceras corniculatum* (Table 1).

2.2 Experimental design, vegetation survey and sample collection

Field surveys and soil samples were conducted during the plant's growing seasons from June to August in 2015–2019. To provide the required spatial heterogeneity, we selected representative wetlands in each coastal city or province with several sampling sites in each independent wetland (Table 1). Based on the plant biogeography and dominant vegetation, we categorized all the sampling sites into six vegetation types, including *P. australis*, *Suaeda*, *P. australis* + *Suaeda*, *S. alterniflora*, mangrove, and tidal flat. Three invasive vegetation types (occurred at sites CI, HI, YB, MRE, JRE, ZRE, ZJ and BH): *P. australis* invaded by *S. alterniflora*, *K. obovata* invaded by *S. alterniflora*, *A. marina* invaded by *S. alterniflora*. Using historical records on the native species composition at each site, we have established that invasive *S. alterniflora* completely outcompeted native *P. australis*. For the native mangrove sites, the invasion had begun along the margin and sparsely populated zones within the mangrove community with the invasion spreading. The invasion by *S. alterniflora* occurred from 7 to 15 years ago, while the native species had been growing at these sites for more than 30 years (Wang et al., 2019). Specifically, the sites with native species were relatively close to their corresponding invaded sites, and we considered SOC contents and soil properties are similar before *S. alterniflora* invasion in paired sites. The vegetation biomasses are shown in Table S1 (our field survey), Table S2 (Yang et al., 2016) and Table S3 (Wang et al., 2019).

Each independent soil was homogenized from three subsamples (within a distance of 20–50 m), and we dispersedly collected several samples from each independent wetland. Samples (from sites LRD, DLJR, NDG and YRE) were collected with an auger at the depths of 0–10, 10–20, 20–30, 30–40, 40–60, 60–80, and 80–100 cm, including a total of 28 sites with 196 samples, while samples (CI, HI, YB, MRE, JRE, ZRE, ZJ and BH) were collected at the depths of 0–10, 10–20, 20–30, and 30–40 cm, including a total of 54 sites with 216 samples. The SOC contents and densities at 60 sites in Jiangsu Province (LRE, SRE, DH, DW, QW, WGW, YCW) and Hainan Province (DB, QH, XH, QH, SYB, SBB, XB, TH, DZ, LG) were obtained from published literature. Together, a total of 142 sites were ultimately obtained. Field samples were divided into two parts. One part was freeze-dried for measuring microbial biomass carbon (MBC), dissolved organic carbon (DOC) and lignin phenols. The other part was air-dried at room temperature in the shade. After removal of the visible stones and root residues, the air-dried soils were gently ground into fine powder, and sieved through a 2 mm and 0.15 mm stainless steel screen to measure soil physico-chemical properties.

2.3 Measurements of soil physico-chemical parameters

2.3.1 Analysis of soil physical parameters

Soil bulk density (BD, g cm^{-3}) was measured using the cutting ring method (100 cm^{-3}). Soil water content (SWC, %) was determined by drying soil samples at 105ºC to constant weight. Soil grain size, defined as clay (< 2 μm), silt (2–20 μm) and sand (>20 μm), were measured by a Mastersizer (3000, Malvern Instruments, Malvern, UK) (Lu, 2000).

2.3.2 Analysis of soil chemical parameters

Soil pH and electrical conductance (EC, μS cm^{-1}) were determined using a pH meter and DDS-307 conductivity analyzer (at a soil to water ratio (w:v) of 1:5; Leici company, Shanghai) (Lu, 2000). DOC (mg kg^{-1}) was extracted with deionized water (w:v = 1:5 ratio), and MBC (mg kg^{-1}) was extracted using the chloroform-fumigation method (Vance et al., 1987), and then measured using a TOC-V_{CPH} analyzer (Shimadzu, Japan). Labile organic carbon (LOC, g kg^{-1}) was extracted with 2.5 M H_2SO_4 and measured by the colorimetric method using a UV-Vis spectrophotometer (UV-2600, Daojin company, Japan; Rovira and Ramón Vallejo, 2007). For total phosphorus (TP, g kg^{-1}) analyses, about 0.03 g soil was melted with lithium metaborate at 950ºC for 0.5 h, then dissolved by 4% (v/v) HNO_3, and measured by the colorimetric method using a UV-Vis spectrophotometer (Ru et al., 2018).

For SOC determination, 0.50 g soil was acidified with 20 mL HCl (1.0 M) for 24 h to remove carbonates, and then washed 3–4 times with distilled water until neutral condition. The total OC and total nitrogen (TN) of the samples were measured using an Elementar Vario EL III (Elementar Analysensysteme, GmnH, Germany).

2.3.3 Analysis of plant-derived lignin phenols

For the determination of plant-derived lignin phenols in soil, 1.00 g soil, 1.00 g copper oxide (CuO), 0.10 g ammonium iron (II) sulfate [$Fe(NH_4)_2(SO_4)_2 \cdot 6H_2O$] and 15 mL of nitrogen (N_2)-purged NaOH (2 mmol L^{-1}) were combined in Teflon-lined bombs. The bombs were flushed with N_2 for about 10 min and heated to 150ºC for 2.5 h in an oven. The lignin oxidation products (LOPs) were derivatized with N, O-bis-(trimethylsilyl) trifluoroacetamide (BSTFA) and pyridine at 70ºC for 3 h to yield trimethylsilyl (TMS) derivatives, and were quantified using internal standards (i.e., trans-Cinnamic acid) on an Agilent 7890B-7010B TQ GC-MS system (Agilent, USA), with separation of derivatized lignin phenols using a DB-5MS column (30 m × 0.25 m × 0.25 μm) (Xia et al., 2021a). Vanillyl, syringyl and cinnamyl (VSC) phenols were summed to represent lignin in soils, and lignin content (Λ_8) was normalized to the OC content to reflect its relative abundance.

2.4 Statistical calculation and analysis

Data were checked for homogeneity of variance and normality before comprehensive analysis. If not, we then performed logarithmic transformation on the data. To utilize and take advantage of all SOC measurements, we used a generalized boosted linear model to obtain the missing data of individual soil properties for a few samples based on the “mice” package by *R* software (www.r-project.org). Data were compared the statistical significance ($p < 0.05$) using a one-way analysis of variance (*ANOVA*). The heatmap of Pearson correlation coefficients was conducted by “ggplot2” package within *R* software. Regression prediction analysis was conducted on the “randomForest” package based on a classification tree to explore the relative influence on SOC contents and density. Data were graphed using Origin 10.0. Variance partitioning analysis (VPA) was conducted using *R* software with the ‘vegan’ package to quantify the explanations of categories of different factors for SOC content and their interactions. The stepwise multiple regression (*SMR*) model was conducted by SPSS 21.0 to assess the variances in SOC content and density explained by different environmental factors.

In this study, we sampled a total of 88 soil profiles, 28 profiles with depths of 0–100 cm (LRD, DLJR, NDG and YRE) and 60 profiles with depths of 0–40 cm (CI, HI, YB, MRE, JRE, ZRE, ZJ and BH). For the 28 profiles with depths of 0–100 cm, we randomly selected 14 profiles as group 1 from the given 28 profiles to build a linear regression equation between the measured SOC density in the 0–40 cm layer and measured SOC density in the 40–60 cm layer ($p < 0.001$; Figure S1A). According to the modeled equation obtained from group 1, we used the measured SOC density in the 0–40 cm layer (group 2) to calculate the predicted SOC density in the 40–60 cm layer of group 2. The differences between the measured density in the 40–60 cm layer (group 2) and the predicted SOC density in the same layer (group 2) were tested using a paired-sample *t*-test ($p < 0.001$; Figure S1B) (Li et al., 2019). Therefore, we consider that the method of the prediction model is reasonable and effective.

Given that, we then established a linear regression equation between the measured SOC density in the 0–40 cm layer and measured SOC density in the 40–60 cm layer based on 28 profiles (group 1 + group 2; Figure S1C). The measured SOC density in the 0–40 cm layer (including sites CI, HI, YB, MRE, JRE, ZRE, ZJ and BH) was used to predict the unknown SOC density in the 40–60 cm layer (CI, HI, YB, MRE, JRE, ZRE, ZJ and BH) based on the prediction model ($y = 0.35x + 3.35$; $R^2 = 0.73$, $p < 0.001$). Similarly, we used the measured SOC density in the 0–60 cm and 0–80 cm layers to calculate the predicted SOC density in the 60–80 cm (Figure S2) and 80–100 cm (Figure S3) layers, respectively ($p < 0.001$). Thus, the 28 soil profiles were used to predict the SOC density in the 40–100 cm layer of 60 soil profiles. For the obtained SOC contents from published literature, we firstly used the formula (Figure 2) to get soil bulk density and then to calculate the SOC density. Similarly, we used the known SOC density to predict the unknown SOC density with corresponding soil layers based on the prediction method.

Calculations of SOC density at national scales in coastal wetlands are obtained primarily in line with four patterns: independent wetlands, vegetation types, invasion types, and climate zones (temperate, subtropical, tropical). We calculated SOC density (SOC_D) for each soil layer as follows (Xiao et al., 2019):

$$SOC_D = \frac{SOC \times BD \times D}{100} \times 10 \qquad (1)$$

where SOC_D is SOC density (Mg C ha^{-1}), SOC represents SOC content (g kg^{-1}), BD is bulk density (g cm^{-3}), and D is soil thickness (cm).

The current SOC sequestration stock was calculated with the following equation:

$$\mathrm{SOCS} = \mathrm{Area} \times SOC_D \qquad (2)$$

where SOCS, Area (Table 1) and SOC_D are SOC sequestration, soil area and SOC density, respectively.

The total inventory of SOC was calculated as follows:

$$TI_{soc} = SOCS_{p1} + SOCS_{p2} + \cdots\cdots SOCS_{pn}$$

where TI_{SOC} represents a total inventory of SOC in the top 1-meter across China's coastal wetlands, $SOCS_{pn}$ represents the current SOC sequestration stock in each coastal province of China.

3 Results

3.1 Relationship between bulk density and soil organic carbon

We established a database with 412 measurements of SOC content and paired bulk density. SOC contents ranged from 0.63 to 36.7 g kg^{-1}, and bulk density was in the range of 0.45–1.87 g cm^{-3}, demonstrating large variability of organic C and physical properties in the coastal wetlands. There was an empirical relationship between measured SOC content and bulk density in the form of $y = -0.47\ln(x) + 2.24$ ($R^2 = 0.72$; $p < 0.001$) (Figure 2).

3.2 Vertical and geographic SOC content distributions

The large standard deviations for vegetation types reflect the wide distribution of vegetation and diversity of wetlands in coastal regions. SOC contents overall decreased with soil depth within the 0–40 cm layer (Figure 3). The wetlands had large spatial differences in SOC contents, with the highest SOC content in the Minjiang River Estuary (23.0 ± 3.94 g kg^{-1}), and the lowest SOC content in the Yellow River Estuary (3.93 ± 1.94 g kg^{-1}). Different sampling sites within the same wetland also displayed some differences in SOC contents (Figure 3A). When grouped by vegetation types, *S. alterniflora* (16.6 ± 4.86 g kg^{-1}) had the highest SOC content, and tidal flat (4.03 ± 1.76 g kg^{-1}) had the lowest SOC content (Figure 3B). When grouped by invasion types, the average SOC content in the native *P. australis* (ΔSOC = -0.51 g kg^{-1}; $p > 0.05$), *K. obovata* (ΔSOC = -2.76 g kg^{-1}; $p < 0.01$) and *A. marina* (ΔSOC = -0.87 g kg^{-1}; $p < 0.01$) communities decreased sharply following *S. alterniflora* invasion (Figure 3C). The measured SOC content was highest in subtropical zones (17.4–20.2 g kg^{-1}), which are 38.5–68.9% and 96.2–155% higher than those in tropical (10.3–14.6 g kg^{-1}) and temperate zones (6.85–10.3 g kg^{-1}), respectively (Figure 3D).

3.3 Comparisons in SOC storage between wetlands or vegetation types

SOC density varied broadly within soil profiles depending on the independent wetland, vegetation type, invasion type, and climatic zone. Different spatial patterns of SOC density for independent wetlands were observed between 20ºN and 40ºN, with relatively higher SOC densities in mid-latitude regions compared to high- and low- latitude regions. The Yellow River Estuary had the lowest SOC densities (28.5–51.7 Mg C ha^{-1}), whereas the Hengsha Island had the highest SOC density (176–202 Mg C ha^{-1}) (Figure 4A).

When grouped by vegetation type, soils with *P. australis* community had the highest OC density (127 Mg C ha^{-1}), being about two times higher than tidal flat (59.5 Mg C ha^{-1}), followed by *S. alterniflora* > mangrove > *P. australis* + *Suaeda* > *Suaeda* > tidal flat (Figure 4B). The average SOC storage in the native *P. australis* community slightly increased following *S. alterniflora* invasion, but in the mangrove community, it markedly decreased compared to the corresponding *S. alterniflora* community, especially in the *K. obovata* community (Figure 4C). We found that wetland SOC density was much higher in subtropical zones than those in the temperate and tropical zones, while the SOC density was similar between the temperate and tropical zones (Figure 4D).

Across the soil profiles, SOC density decreased with depth in the 0–40 cm layer, but displayed no significant decrease in the 40–100 cm layer. This suggests that SOC is more reactive or labile in topsoil than in subsoil/deeper soil, probably related to the root system distribution and rhizodeposits in soil profile. In the past, the IPCC (2003) recommended a soil depth of 30 cm for the assessment of SOC density in response to global climate change.

However, we found that only 40% of the organic C was stored in the top 30 cm, and the majority of the soil C stocks was partitioned in the 30–100 cm layer regardless of the location of wetland, types of vegetation, vegetation invasion, and climate-zone (Figure 4), suggesting that the deeper OC should be also considered in OC stock assessment.

3.4 Correlations between environmental variables and SOC content under different scenarios

For independent wetlands, the Pearson correlations showed that SOC contents were largely different and were significantly correlated to various edaphic variables (Figure 5A), suggesting a large spatial heterogeneity of soil properties for the location of each coastal wetland. For the three climatic zones, the significant differences between SOC content and edaphic variables were BD, clay and MBC (Figure 5B). Both TN and BD were the common factors affecting SOC content for soils with different vegetation, while the other soil parameters were a variant for each vegetation type (Figure 5C). We found that the correlations between SOC content and edaphic variables were strongly altered following *S. alterniflora* invasion of native species (*P. australis*, *K. obovata*, *A. marina*). For example, the particle size composition (clay, silt and sand) was significantly correlated to SOC content for soils with *S. alterniflora* vegetation, but not for *P. australis* vegetation (Figure 5D). The correlations between climatic factors (MAT and MAP) and SOC density was best described using a cubic function, and the relationships in 0–40 cm layer were more prominent than in 40–100 layer (Figure 6).

3.5 Environmental controls on SOC content and density

We conducted variance partitioning analysis (VPA) using two categories (soil properties and climate), soil properties solely explained 29% of the variance, and climate only explained 3% of the variance for SOC content, while soil properties and climate had the largest interactive effects (42%; Figure 7A). Then, the results of the VPA using three categories (soil chemical properties, physical properties and climate) showed that soil chemical properties were the most important variable explaining SOC content (59% of the variation), while soil physical properties (15%) only accounted for a small proportion (Figure 7B).

In determining the relative importance of soil factors on SOC content and density, random forest analysis was carried out and the results demonstrated edaphic variables were in the order TN > BD > TP > $(Ad/Al)_V$ > MBC > pH > SWC > EC > DOC > clay > silt > sand > S/V > $(Ad/Al)_S$ ($p < 0.05$; Figure 8A), while for SOC density followed the order of TN > EC > SWC > MBC > TP > DOC > pH > sand > silt > sand > $(Ad/Al)_V$ ($p < 0.05$; Figure 8B). However, Λ_8 (reflecting plant C inputs into soil) was not a significant factor influencing SOC content and density.

Stepwise multiple regression analysis was used to assess the combined effects of soil physical, chemical properties, biological traits (i.e., plant-derived lignin phenols) and climatic factors on SOC content. The extracted factors explained more than 90% of the variation in the SOC content. For the extracted parameters based on these analyses of different classification basis, soil chemical properties were the dominant factor controlling SOC content, followed by soil physical properties. Biological traits were a minor contributor to regulating SOC content, and MAP and MAT only exerted effects under specific regions with a large latitude span (Table 2).

4 Discussion

4.1 SOC inventories in China's coastal wetlands

Our dataset here represents the most comprehensive assessment of measured organic C density and sequestration inventory of coastal wetlands in China. Our study utilized 100 cm as an ideal sampling depth to identify the SOC density and sequestration stock (Howard et al., 2017), thereby capturing both the more dynamic organic C in the surface soil and the more stable C stocks in the subsoil. Previous studies have demonstrated that SOC density varied widely depending on wetland types (Xiao et al., 2019) and locations (Nahlik and Fennessy, 2016), with higher C stocks under lower temperature and anaerobic conditions (Lee et al., 2018). As such, we have carried out a more detailed division of coastal wetlands, including the location of independent wetland, vegetation composition, invasion type and climatic zone, to more accurately quantify the C stocks in coastal wetlands of China.

We found a wide range of SOC densities, ranging from about 40 to 200 Mg C ha^{-1}. VPA results likely showed that the diversity of precipitation and temperature in different climatic regions (temperate, subtropical and tropical) contributed to these substantial variations on long time-scales (Figure 7; Osland et al., 2018). The results showed that the Yellow River Estuary had the lowest SOC content and density across the national scale. This system had the highest sand content reinforcing the notion that grain size plays an important role in aggregate stabilization and C sequestration capacity in global coastal wetlands (Yu et al., 2021). The differing contribution of autochthonous vs. allochthonous C inputs is also likely to vary spatially because of differences in local hydrological conditions, wetland management and vegetation in the catchment (Saintilan et al., 2013). Autochthonous inputs mainly include plant aboveground litter, root residues and their secretions, primary and secondary products of phytoplankton and benthos; while allochthonous inputs mainly include particulate organic carbon (POC) and dissolved organic carbon (DOC) carried by the processes of tidal inundation, surface runoff and groundwater (Saintilan et al., 2013; Xia et al., 2021a). This highlights the importance of both broad and small spatial-scale data in understanding differences in C stocks under natural scenarios and estimating regional wetland C stocks. The soil C densities of coastal wetlands in China were basically close to the values (93.7 Mg ha^{-1}) reported by Xiao et al. (2019), but lower than those reported for coastal wetlands in USA (300 Mg ha^{-1}) (Nahlik and Fennessy, 2016) are higher than ours.

4.2 Factors affecting SOC distribution patterns

4.2.1 Climatic influences

Temperature and moisture control net primary productivity which influences inputs (detritus and rhizodeposits) of OC, as well as SOC decomposition (Jobbágy and Jackson, 2010). Hilasvuori et al. (2013) have reported that temperature is the primary factor affecting the accumulation and decomposition of SOC in wetlands of Central Finland. Increased temperature stimulates the loss of organic C pools, especially in high latitudes (Clair et al., 2002; Inglett et al., 2012), thus stressing the risk of SOC loss under a warming climate (Bond-Lamberty and Thomson, 2010). SOC density in tropical zones (i.e., Zhanjiang and Beihai) was generally lower than that in subtropical areas (Figure 4D), most likely due to higher rates of SOC decomposition in the former. The difference of SOC density of each layer in subsoil (40–100 cm) is much lower than that in topsoil (0–40 cm), we assumed that SOC density in the subsoil is relatively more stable compared to topsoil across the three climate zones. However, Li et al. (2020) demonstrated that SOC in subsoil in forest ecosystems is likely to be more vulnerable than in topsoil under rising temperatures, and this phenomenon was primarily controlled by climate and soil C quality. We consider that changing climate will have different effects on SOC stocks based on whether the soils are from upland and wetland. The availability of water (i.e., high water content or shallow water table) in soils can be strongly affected by hydrological dynamics and soil porosity, which may largely restrict oxygen availability for microbes to utilize SOC and soil thermal regimes (Luo et al., 2020). As such, the response of the soil C pool to temperature in wetlands is also influenced by abiotic processes of soil itself, including water availability, nutrient input, and oxygen supply (Olefeldt and Roulet, 2012). The VPA showed soil properties and climate had the largest interactive effects (42%; Figure 7A). This further revealed that other physical and chemical factors, such as temperature, could also affect the mineralization of OC pools by microorganisms (Villa and Bernal, 2018).

High precipitation and temperature are usually coupled with high plant productivity (Beer et al., 2010), thus influencing plant C inputs into soil, which interacts with inundation periods and depths. In addition, climate can have a direct effect on soil texture, chemical properties and mineralogy, which are closely linked with SOC turnover (Luo et al., 2017). A recent study focusing on the main driving factors controlling C cycling suggested that soil properties (e.g., soil clay content and C:N ratio) rather than climate control the vertical variations of SOC, microbial biomass carbon, and microbial metabolic quotient (Sun et al., 2020). In other words, the sensitivity of SOC dynamics to climate variability may be buffered by changes in primary productivity and soil properties. Our results demonstrate the importance of the interactions between climate, soil, and the amounts and quality of C input (Figure 7; Figure S4). Because of the complex processes involved in forming organic C under different climate conditions, further studies on the trade-off or net effect between primary productivity and soil C decomposition are justified (Bradford et al., 2016). However, to fully consider the influence of all factors on SOC dynamics, previous studies often incorporate climate factors with plant biomass as well as soil properties into one model, which will overestimate the impact of climate on SOC dynamics. This clearly needs further attention and warrants in-depth studies (i.e., geological and tidal information) in the future.

4.2.2 Vegetation composition and exotic plant invasion

The quantity and quality of C inputs are strongly affected by vegetation type, which is predominantly controlled by climatic conditions and interacts with soil conditions (Beer et al., 2010; Luo et al., 2017). Different plant communities can influence OC sequestration rates within each vegetation type (Mitsch et al., 2013; Villa and Mitsch, 2015). Researchers often take it for granted that SOC stocks are high under vegetation communities with high net primary productivity (NPP). While it is established that NPP influences C inputs into soil, its effect on SOC stock, particularly in deeper soil layers, is minimal (Figure 4). In other words, it may largely depend on how much biomass ends up in soils, transformation pathways to SOM, priming effects and transportation to deeper soil layers. Thus, NPP may not be a useful indicator of C inputs, especially in deeper soil layers (Xiao et al., 2019). Subsoils may be subject to greater environmental controls than topsoil, including water logging and anoxic conditions. These environmental conditions may result in more complex SOC stabilization processes and a divergent behavior in the decomposer community (Keiluweit et al., 2017), lessening the influence of NPP on SOC stock in deeper soil layers. Therefore, the difference in SOC stocks in subsoil among vegetation types was less than that in topsoil (Figure 4). The relatively minor role of plant C inputs (Λ_8; $p > 0.05$) in determining the spatial distribution of SOC content and density (Figure 8), however, does not signify less important factor for local C management. Under similar climatic and edaphic conditions, as the mixed vegetation of *P. australis* and *Suaeda*, *Suaeda* alone had lower NPP (Figure 9), thus lower inputs of SOC compared to other vegetation types.

The influence of plant C inputs is straightforward as C influx to soil directly determines OC content. The quality of C inputs (e.g., lignin, C:N, and lignin: N) influences OC utilization by microorganisms and their utilization strategies (Bending et al., 2002; Cotrufo et al., 2013). This in turn controls the composition, preservation, and distribution of SOC pools and their decomposability as a cohort (Prescott, 2010; Raich and Tufekciogul, 2000). SOC content and density in woody mangrove (*K. obovata* and *A. marina*) sharply decreased following the herbaceous *S. alterniflora* invasion (Figure 3C & 4C). Litters from above- and below-ground components in mangrove forests tend to have greater recalcitrant C compounds (e.g., lignin, tannins, cutin, suberin, and waxes) and are more difficult to decompose than those from invasive *S. alterniflora* (Chanda et al., 2015). More importantly, soils or sediments tend to efficiently sequester organic C in mangrove forests, which is attributed to the morphological structure of mangroves and their widespread density and distribution of roots (Krauss et al., 2003). The unique tree structure and complex aerial root systems (e.g., prop roots and pneumatophores) across mangrove species could result in greater biomasses than grasses, and these specific root structures are more effective for trapping organic-rich sediments (Kristensen et al., 2008). For two herbaceous plants, SOC density in native *P. australis* community slightly increased following *S. alterniflora* invasion (Figure 4C). We mainly attributed this result to the following three reasons: (i) the decomposition rate of *S. alterniflora* litter, particularly the belowground root residues, was slower than that of *P. australis* litter due to the lower litter quality (i.e., higher C:N ratio) of *S. alterniflora* (Liao et al., 2008; Duan et al., 2018); (ii) the biomass of *S. alterniflora* was higher than that of *P. australis* (Wang et al., 2019); (iii) *S. alterniflora* grew closer to the coast and estuary in comparison to *P. australis*.

However, the SOC density in wetlands predominantly vegetated by mangroves (e.g., southern China from south-central Zhejiang to Hainan Province) is not the largest despite having the highest biomass and the percent of recalcitrant C components (Xia et al., 2021b). The net SOC density is dependent not only on the apparent NPP and litters (Figure 9), but largely on how much of the apparent NPP and litters eventually enters the soil, and how SOC is eventually preserved and stabilized in environments. In addition, plant/litterfall lateral export or import via tidal water also might be the key process to influencing SOC accumulation.

4.2.3 Soil properties

The stabilization mechanisms of SOC have been intensively discussed with respect to (i) physical protection by aggregates associated with minerals, (ii) the nature of recalcitrant compounds of SOC, and (iii) refractory biological components (such as microbial residual carbon), and cementation of physicochemical function and biological substances (Cui et al., 2014; Throckmorton et al., 2015; Sarker et al., 2018). These SOC stabilization mechanisms have been demonstrated in uplands to increase C sequestration (Fujisaki et al., 2018; Wang et al., 2015; Poeplau et al., 2017; Luo et al., 2017; Sarker et al., 2018). Less attention, however, has been paid to understanding the mechanisms of soil C stabilization in coastal wetlands at large regional scale, and investigations on the relative influence of individual soil properties remain scarce.

VPA showed that soil chemical properties were more important than physical properties in controlling SOC content (Figure 7B). Also, stepwise multiple regression analysis showed that the quality of C fractions and nutrients are the most important factors for SOC content (Table S4 & S5). However, increasing evidence suggests that physical protection plays an important role in the preservation of SOC and chemical make-up is less important in uplands (Ekschmitt et al., 2008; Kleber et al., 2011; Guo et al., 2018). We attributed these differences in preservation to (i) OC with recalcitrant compounds is decomposable in uplands at the time scale from years to decades (Fontaine et al., 2007; Schmidt et al., 2011), and (ii) coastal wetlands are in the intertidal zones or permanently flooded environments.

In detail, we found clay is an important parameter influencing SOC content in tidal flats, and this is consistent with studies of Lehmann et al. (2007) and Dungait et al. (2012), showing that clay content is an important factor in controlling SOC dynamics in salt marshes. For the *K. obovata* community, SOC content significantly decreased following *S. alterniflora* invasion, and C/V was the most important parameter controlling SOC content (Table S4). High contents of plant-derived lignin phenols were found in mangrove soils (Supplementary original data). Recalcitrant organic C was reported to be a major proportion of SOC in an estuarine ecosystem in southern China (Lian et al., 2018). In the *A. marina* community, silt content is considered as a pivotal parameter, and this is also consistent with the study of Xiong et al. (2018) showing that SOC content was primarily controlled by the proportion of finer soil particles in a mangrove ecosystem. For *S. alterniflora* community, both $(Ad/Al)_V$ and $(Ad/Al)_S$ were important factors controlling SOC content, and suggested SOC molecular composition exerted important roles in protecting from decomposition. Sun et al. (2019) have reported that the simpler OC molecular structure (higher ratio of alkyl C to O-alkyl C and lower aromaticity) of *S. alterniflora* soils hindered the accumulation of SOC compared with mangrove. Therefore, intrinsic SOC stabilization such as chemical protection possibly plays a significant role in controlling SOC dynamics and turnover.

One study reported that organo-mineral association was the major mechanism of SOC stabilization in salt marshes, recalcitrant C (as indicated by relatively high aromaticity and low mineral OC) in mangrove soil contributes to SOC stabilization (Sun et al., 2019). Future studies should strengthen the understanding of the role of mineral (i.e., iron, aluminum, calcium compounds) association in SOC stabilization, and help quantifying the relative importance of mineral association vs. chemical protection in SOC stabilization in coastal ecosystems at large-regional scales.

4.3 Comparisons of SOC density in coastal wetlands with inland wetlands

Based on the geographic locations, hydrological conditions and salinity, researchers often categorized the wetlands as: river, coastal, lake and marsh (Figure 10; State Forestry Administration, 2015). SOC density of these wetland types generally decreased in the order of marsh > lake > river > coastal. Marsh wetlands store the most C, and are mainly distributed in the northeast China and Qing-Tibetan Plateau regions, most likely reflecting high litter inputs/preservation, cool temperatures and relatively anaerobic conditions which minimize C mineralization and favor C accumulation (Lin et al., 2013). Lakes also promote C accumulation because they are mostly closed basins that stabilize C and transport little C from surrounding environments (Euliss et al., 2014; Pennock et al., 2010). By contrast, river wetlands are 'neutral pipes' for C accumulation that merely convey landward C to oceans, and mostly accept particulate organic carbon and dissolved organic carbon from upstream (Cole et al., 2007; Aufdenkampe et al., 2011). Compared to inland wetlands, coastal wetlands are adjacent to the landward and ocean. Plant productivity is usually low under saline conditions and long-term flooded environments with high water-level. Mild climatic conditions enhance the decomposition of OC thus limiting the potential for C storage, because coastal wetlands would be exposed to air at low tide and subjected to alternating wet-dry environment (Moinet et al., 2018), even though, they are generally believed to have the highest C store among terrestrial ecosystem worldwide (Lu et al., 2017). Coastal wetlands are open ecosystems, and the different roles of inland and coastal wetlands in C accumulation are interesting and need further study. Wetland types (marsh, lake, coastal, and river) were examined to gain a better understanding of their roles in contributing to SOC sequestration.

4.4 Implications for blue C management in coastal wetlands

Coastal wetlands are open ecosystems at the land and ocean interface, which are more prone to be influenced by anthropogenic activities, rising sea-level, hydrogeological conditions, and river runoff (Rogers et al., 2014; Meng et al., 2017). The multifunctional and complex roles of organic C in these systems remain largely unstudied, in particular relating to the storage, and factors controlling the storage of blue C. Marsh wetlands are mainly distributed in inland regions (Northeast China and Qing-Tibetan Plateau), and contain the largest C pool. However, the coastal regions are at greater risk of being utilized for agricultural and industrial purposes, thus resulting in accelerated decomposition and release of stored organic C (O’Connor et al., 2019). Therefore, salt marshes (such as Liao River Delta) are one of the primary focuses for wetland C managements in China. The salinity, redox state and nutrient content (particularly TN and TP) of the wetlands can be affected by climate change and anthropogenic activities including development, tillage, drainage. Treating these variables as a constant may result in poor quantification of SOC stocks (Table S4). Eutrophication and pollution are the main problems threatening ecological health of river and lake wetlands (Beaulieu et al., 2019). Comprehensive protection measures are needed to strengthen supervision and administration of environmental protection in river and lake basins, and to reduce the discharge of pollutants from industrial and domestic wastewaters, thus maintaining the environmental status and C budgets of river and lake wetlands (Xiao et al., 2019). Additionally, land use change and intensity (i.e., coastal wetland restoration, harvest of wetland macrophytes, and frequency of tides) should be fully considered, which may significantly affect SOC stabilization processes and thus SOC stocks in managed areas. If these processes are fully addressed, improved predictions as well as increased blue C accumulation are possible, providing significant opportunities to contribute to climate change mitigation.

4.5 Uncertainties in C sequestration and outlooks

While our study provides a vast and comprehensive dataset of SOC stocks and their controlling factors in wetlands across climate gradient, vegetation composition and invasion types, there are still limitations and uncertainties in the datasets and assessment. Firstly, most of China's coastal wetland area data were taken from literature, and current data sources are derived from the national soil census (Zheng et al., 2013), local investigation reports (Ding et al., 2004), and remote sensing data (Ma et al., 2015). The above data used for calculating C sequestration in wetlands are inconsistent in data acquisition. Secondly, although our sampling sites in coastal wetlands were representative and decentralized, more sampling sites could be added to further strengthen the statistical significance. Thirdly, there are diverse types with a large amount of different dominant plants (Figure 10), even within the same wetland in the whole coastal wetlands, the categorization was based on our investigations and subjectivity (Table 1). Fourthly, depths of wetland soils varied significantly and there are several examples from our data showing that sampling even to 100 cm may not truly represent the C storage potential of these systems. However, data for soil depths were unavailable in some sites. Due to the lack of these reliable data, we used the existing soil C stocks (0–100 cm) to predict other sites (40–100 cm). The model estimation methods might over- or under- estimate C stocks in China's coastal wetlands. Although our results of C stocks here were obtained based on multisource data, new calculations here are effective to reflect the whole picture of organic C distributions at a national scale.

5 Conclusions

Coastal wetlands play an important role in C sequestration, and at the same time they are sensitive to climate change and anthropogenic disturbances. Although high precipitation and temperature conditions usually result in high plant productivity and thus higher C inputs into soil, wetland SOC density are not simply correlated with MAT and MAP. Changes in SOC density under vegetation communities were not completely consistent with NPP. This was attributed to differences in SOC decomposition/preservation, litter inputs, and the quality of SOC. We calculated a total inventory of 57 $\times 10^6$ Mg C in the top 1-meter soil in coastal wetlands of China. Edaphic variables solely override climate control of SOC content, chemical make-up (i.e., the nature of recalcitrant compounds) plays more important role in the preservation of SOC than physical protection. Soil chemical properties exert strong interactive effects with climate. Plant biological traits were a minor contributor in regulating SOC content. Random forest analysis results showed that the relative importance of predictor variables was in the order of TN > BD > TP > (Ad/Al)v > MBC > pH > SWC > EC> DOC > Clay > Silt > and > S/V >Λ_8 for SOC contents, and with the order of TN > EC > SWC > MBC > TP > DOC > pH > Sand > Silt > Clay > (Ad/Al)v for SOC density. Knowledge and information gained have important implications for understanding mechanisms in SOC stabilization and sequestration capability, and will aid policy and decisions concerning vegetation cover and environmental management, thus contributing to global efforts to mitigate climate change.

Acknowledgements

This study was financially supported by the National Natural Science Foundation of China (Grant Nos. 42141014 and 41930862), Natural Science Foundation of Jiangsu Province (Grant Nos. BK20221028), and the State's Key Project of Research and Development Plan of China (Grant Nos. 2016YFA0601002 and 2017YFC0212700). Financial support was also provided by the Haihe Laboratory of Sustainable Chemical Transformations.

Conflict of interest

All authors declare no conflict of interests.

Data availability statement

The data that support this study are available in the Supplementary materials, and the supplementary original data would be open access for researchers in figshare webpage https://figshare.com/articles/dataset/Supplementary_original_data_for_Storage_patterns_and_influencing_factors_for_soil_organic_carbon_in_coastal_wetlands_of_China_/20180450.

References

Atwood, T. B., Connolly, R. M., Almahasheer, H., Carnell, P. E., Duarte, C. M., Ewers Lewis, C. J., … Lovelock, C. E. (2017). Global patterns in mangrove soil carbon stocks and losses. *Nature Climate Change*, *7*(7), 523–528. https://doi.org/10.1038/nclimate3326

Aufdenkampe, A. K., Mayorga, E., Raymond, P. A., Melack, J. M., Doney, S. C., & Alin, S. R., et al. (2011). Riverine coupling of biogeochemical cycles between land, ocean and atmosphere. *Frontiers in Ecology and the Environment, 9*(1), 53-60. https://doi.org/10.1890/100014

Bahadori, M., Chen, C., Lewis, S., Boyd, S., Rashti, M. R., Esfandbod, M., ... & Kuzyakov, Y. (2021). Soil organic matter formation is controlled by the chemistry and bioavailability of organic carbon inputs across different land uses. *Science of The Total Environment*, *770*, 145307. https://doi.org/10.1016/j.scitotenv.2021.145307

Beaulieu, J. J., DelSontro, T., & Downing, J. A. (2019). Eutrophication will increase methane emissions from lakes and impoundments during the 21st century. *Nature Communications*, *10,* 1375. https://doi.org/10.1038/s41467-019-09100-5

Beer, C., Reichstein, M., Tomelleri, E., Ciais, P., Jung, M., Carvalhais, N., . . . Bondeau, A. (2010). Terrestrial gross carbon dioxide uptake: Global distribution and covariation with climate. *Science*, *329*, 834–838. https://doi.org/10.1126/science.1184984

Belyea, L. R., & Malmer, N. (2004). Carbon sequestration in peatland: patterns and mechanisms of response to climate change. *Global Change Biology*, *10*(7), 1043–1052. https://doi.org/10.1111/j.1529-8817.2003.00783.x

Bending, G. D., Turner, M. K., & Jones, J. E. (2002). Interactions between crop residue and soil organic matter quality and the functional diversity of soil microbial communities. *Soil Biology and Biochemistry*, *34*(8), 1073–1082. https://doi.org/10.1016/s0038-0717(02)00040-8

Bernal, B., & Mitsch, W. J. (2012). Comparing carbon sequestration in temperate freshwater wetland communities. *Global Change Biology*, *18*(5), 1636–1647. https://doi.org/10.1111/j.1365-2486.2011.02619.x

Bond-Lamberty, B., & Thomson, A. (2010). Temperature-associated increases in the global soil respiration record. *Nature*, *464*(7288), 579–582. https://doi.org/10.1038/nature08930

Bradford, M. A., Wieder, W. R., Bonan, G. B., Fierer, N., Raymond, P. A., & Crowther, T. W. (2016). Managing uncertainty in soil carbon feedbacks to climate change. *Nature Climate Change*, *6*(8), 751–758. https://doi.org/10.1038/nclimate3071

Carvalhais, N., Forkel, M., Khomik, M., Bellarby, J., Jung, M., Migliavacca, M., … Reichstein, M. (2014). Global covariation of carbon turnover times with climate in terrestrial ecosystems. *Nature*, *514*(7521), 213–217. https://doi.org/10.1038/nature13731

Chanda, A., Akhand, A., Manna, S., Das, S., Mukhopadhyay, A., Das, I., … Dadhwal, V. K. (2015). Mangrove associates versus true mangroves: a comparative analysis of leaf litter decomposition in Sundarban. *Wetlands Ecology and Management*, *24*(3), 293–315. https://doi.org/10.1007/s11273-015-9456-9

Chen, H., Zhu, Q., Peng, C., Wu, N., Wang, Y., Fang, X., … Wu, J. (2013). The impacts of climate change and human activities on biogeochemical cycles on the Qinghai-Tibetan Plateau. *Global Change Biology*, *19*(10), 2940–2955. https://doi.org/10.1111/gcb.12277

Clair, T., Arp, P., Moore, T., Dalva, M., & Meng, F. R. (2002). Gaseous carbon dioxide and methane, as well as dissolved organic carbon losses from a small temperate wetland under a changing climate. *Environmental Pollution*, *116*, S143–S148. https://doi.org/10.1016/s0269-7491(01)00267-6

Cole, J. J., Prairie, Y. T., Caraco, N. F., McDowell, W. H., Tranvik, L. J., Striegl, R. G., … Melack, J. (2007). Plumbing the global carbon cycle: Integrating inland waters into the terrestrial carbon budget. *Ecosystems*, *10*, 172–185. https://doi.org/10.1007/s10021-006-9013-8

Cotrufo, M. F., Wallenstein, M. D., Boot, C. M., Denef, K., & Paul, E. (2013). The Microbial Efficiency-Matrix Stabilization (MEMS) framework integrates plant litter decomposition with soil organic matter stabilization: do labile plant inputs form stable soil organic matter? *Global Change Biology*, *19*(4), 988–995. https://doi.org/10.1111/gcb.12113

Cui, J., Li, Z., Liu, Z., Ge, B., Fang, C., Zhou, C., & Tang, B. (2014). Physical and chemical stabilization of soil organic carbon along a 500-year cultived soil chronosequence originating from estuarine wetlands: Temporal patterns and land use effects. *Agriculture, Ecosystems & Environment*, *196*, 10-20. https://doi.org/10.1016/j.agee.2014.06.013

Davidson, E. A., & Janssens, I. A. (2006). Temperature sensitivity of soil carbon decomposition and feedbacks to climate change. *Nature*, *440*(7081), 165–173. https://doi.org/10.1038/nature04514

Ding, W., Cai, Z., & Wang, D. (2004). Preliminary budget of methane emissions from natural wetlands in China. *Atmospheric Environment*, *38*(5), 751–759. https://doi.org/10.1016/j.atmosenv.2003.10.016

Duan, H., Wang, L., Zhang, Y., Fu, X., Tsang, Y., Wu, J., & Le, Y. (2018). Variable decomposition of two plant litters and their effects on the carbon sequestration ability of wetland soil in the Yangtze River estuary. *Geoderma*, *319*, 230-238. https://doi.org/10.1016/j.geoderma.2017.10.050

Duan, X., Yu, X., Li, Z., Wang, Q., Liu, Z., & Zou, Y. (2020). Iron-bound organic carbon is conserved in the rhizosphere soil of freshwater wetlands. *Soil Biology and Biochemistry*, *149*, 107949. https://doi.org/10.1016/j.soilbio.2020.107949

Duarte, C. M., Losada, I. J., Hendriks, I. E., Mazarrasa, I., & Marbà, N. (2013). The role of coastal plant communities for climate change mitigation and adaptation. *Nature Climate Change*, *3*(11), 961–968. https://doi.org/10.1038/nclimate1970

Dungait, J. A. J., Hopkins, D. W., Gregory, A. S., & Whitmore, A. P. (2012). Soil organic matter turnover is governed by accessibility not recalcitrance. *Global Change Biology*, *18*(6), 1781–1796. https://doi.org/10.1111/j.1365-2486.2012.02665.x

Ekschmitt, K., Kandeler, E., Poll, C., Brune, A., Buscot, F., Friedrich, M., ... & Wolters, V. (2008). Soil-carbon preservation through habitat constraints and biological limitations on decomposer activity. *Journal of Plant Nutrition and Soil Science*, *171*(1), 27-35. https://doi.org/10.1002/jpln.200700051

Euliss, N. H., Mushet, D. M., Newton, W. E., Otto, C. R. V., Nelson, R. D., LaBaugh, J. W., … Rosenberry, D. O. (2014). Placing prairie pothole wetlands along spatial and temporal continua to improve integration of wetland function in ecological investigations. *Journal of Hydrology*, *513*, 490–503. https://doi.org/10.1016/j.jhydrol.2014.04.006

Feng, W., Plante, A. F., & Six, J. (2013). Improving estimates of maximal organic carbon stabilization by fine soil particles. *Biogeochemistry*, *112*(1-3), 81–93. https://doi.org/10.1007/s10533-011-9679-7

Fontaine, S., Barot, S., Barré, P., Bdioui, N., Mary, B., & Rumpel, C. (2007). Stability of organic carbon in deep soil layers controlled by fresh carbon supply. *Nature*, *450*(7167), 277-280. https://doi.org/10.1038/nature06275

Friborg, T., Soegaard, H., Christensen, T. R., Lloyd, C. R., & Panikov, N. S. (2003). Siberian wetlands: where a sink is a source. *Geophysical Research Letters*, *30*(21), 2129-2133. https://doi.org/10.1029/2003GL017797

Fu, C. C., Li. Y., Zeng, L., Zhang, H. B., Tu, C., Zhou, Q., et al. (2021). Stocks and losses of soil organic carbon from Chinese vegetated coastal habitats. *Global Change Biology*, *27*, 202–214. https://doi.org/10.1111/gcb.15348

Fujisaki, K., Chapuis-Lardy, L., Albrecht, A., Razafimbelo, T., Chotte, J. L., & Chevallier, T. (2018). Data synthesis of carbon distribution in particle size fractions of tropical soils: Implications for soil carbon storage potential in croplands. *Geoderma*, *313*, 41-51. https://doi.org/10.1016/j.geoderma.2017.10.010

Gao, Y., Peng, R., Ouyang, Z., Shao, C., Chen, J., Zhang, T., … Zhao, B. (2020). Enhanced lateral exchange of carbon and nitrogen in a coastal wetland with invasive *Spartina alterniflora. Journal of Geophysical Research: Biogeosciences*, e2019JG005459. https://doi.org/10.1029/2019jg005459

Gao, Y., Zhou, J., Wang, L., Guo, J., Feng, J., Wu, H., & Lin, G. (2019). Distribution patterns and controlling factors for the soil organic carbon in four mangrove forests of China. *Global Ecology and Conservation*, *17*, *e00575*. https://doi.org/10.1016/j.gecco.2019.e00575

Guo, J., Wang, B., Wang, G., Wu, Y., & Cao, F. (2018). Vertical and seasonal variations of soil carbon pools in ginkgo agroforestry systems in eastern China. *Catena*, *171*, 450-459. https://doi.org/10.1016/j.catena.2018.07.032

Han, G., Tang, Y., Liu, M., Van Zwieten, L., Yang, X., Yu, C., ... & Song, Z. (2020). Carbon-nitrogen isotope coupling of soil organic matter in a karst region under land use change, Southwest China. *Agriculture, Ecosystems & Environment*, *301*, 107027. https://doi.org/10.1016/j.agee.2020.107027

Hayes, M. A., Jesse, A., Hawke, B., Baldock, J., Tabet, B., Lockington, D., & Lovelock, C. E. (2017). Dynamics of sediment carbon stocks across intertidal wetland habitats of Moreton Bay, Australia. *Global Change Biology*, *23*(10), 4222–4234. https://doi.org/10.1111/gcb.13722

Hicks Pries, C. E., Castanha, C., Porras, R. C., & Torn, M. S. (2017). The whole-soil carbon flux in response to warming. *Science*, *355*(6332), 1420–1423. https://doi.org/10.1126/science.aal1319

Hilasvuori, E., Akujärvi, A., Fritze, H., Karhu, K., Laiho, R., Mäkiranta, P., … Liski, J. (2013). Temperature sensitivity of decomposition in a peat profile. *Soil Biology and Biochemistry*, *67*, 47–54. https://doi.org/10.1016/j.soilbio.2013.08.009

Hinson, A. L., Feagin, R. A., Eriksson, M., Najjar, R. G., Herrmann, M., Bianchi, T. S., … Boutton, T. (2017). The spatial distribution of soil organic carbon in tidal wetland soils of the continental United States. *Global Change Biology*, *23*(12), 5468–5480. https://doi.org/10.1111/gcb.13811

Hopkinson, C. S., Cai, W.-J., & Hu, X. (2012). Carbon sequestration in wetland dominated coastal systems – A global sink of rapidly diminishing magnitude. *Current Opinion in Environmental Sustainability*, *4*(2), 186–194. https://doi.org/10.1016/j.cosust.2012.03.005

Howard, J., Sutton-Grier, A., Herr, D., Kleypas, J., Landis, E., Mcleod, E., … Simpson, S. (2017). Clarifying the role of coastal and marine systems in climate mitigation. *Frontiers in Ecology and the Environment*, *15*(1), 42–50. https://doi.org/10.1002/fee.1451

Inglett, K. S., Inglett, P. W., Reddy, K. R., & Osborne, T. Z. (2012). Temperature sensitivity of greenhouse gas production in wetland soils of different vegetation. *Biogeochemistry, 108*(1-3), 77-90. https://doi.org/10.1007/s10533-011-9573-3

Jiao, N., Liang, Y., Zhang, Y., Liu, J., Zhang, Y., Zhang, R., … Zhang, S. (2018). Carbon pools and fluxes in the China Seas and adjacent oceans. *Science China Earth Sciences*. https://doi.org/10.1007/s11430-018-9190-x

Jobbágy, E. G., & Jackson, J. R. B. (2000). The vertical distribution of soil organic carbon and its relation to climate and vegetation. *Ecological Applications, 10*(2), 423-436. https://doi.org/10.1890/1051-0761(2000)010[0423:tvdoso]2.0.co;2

Keiluweit, M., Wanzek, T., Kleber, M., Nico, P., & Fendorf, S. (2017). Anaerobic microsites have an unaccounted role in soil carbon stabilization. *Nature Communications*, *8*, 1771. https://doi.org/10.1038/s41467-017-01406-6

Kirwan, M. L., & Megonigal, J. P. (2013). Tidal wetland stability in the face of human impacts and sea-level rise. *Nature, 504*(7478), 53–60. https://doi.org/10.1038/nature12856

Kleber, M., Nico, P. S., Plante, A., Filley, T., Kramer, M., Swanston, C., & Sollins, P. (2011). Old and stable soil organic matter is not necessarily chemically recalcitrant: implications for modeling concepts and temperature sensitivity. *Global Change Biology*, *17*(2), 1097-1107. https://doi.org/10.1111/j.1365-2486.2010.02278.x

Krauss, K. W., Allen, J. A., & Cahoon, D. R. (2003). Differential rates of vertical accretion and elevation change among aerial root types in Micronesian mangrove forests. *Estuarine, Coastal and Shelf Science*, *56*(2), 251-259. https://doi.org/10.1016/S0272-7714(02)00184-1

Kristensen, E., Bouillon, S., Dittmar, T., & Marchand, C. (2008). Organic carbon dynamics in mangrove ecosystems: a review. *Aquatic Botany*, *89*(2), 201-219. https://doi.org/10.1016/j.aquabot.2007.12.005

Lal, R. (2004). Soil carbon sequestration impacts on global climate change and food security. *Science*, 304, 1623–1627. https://doi.org/10.1126/science.1097396

Lal, R. (2008). Carbon sequestration. *Philosophical Transactions of the Royal Society of London*, *363*, 815–830. https://doi.org/10.1098/rstb.2007.2185

Lee, C. G., Suzuki, S., & Inubushi, K. (2018). Temperature sensitivity of anaerobic labile soil organic carbon decomposition in brackish marsh. *Soil Science and Plant Nutrition*, *64*(4), 443–448. https://doi.org/10.1080/00380768.2018.1464374

Lehmann, J., & Kleber, M. (2015). The contentious nature of soil organic matter. *Nature*, *528*, 60–68. https://doi.org/10.1038/nature16069

Lehmann, J., Kinyangi, J., & Solomon, D. (2007). Organic matter stabilization in soil microaggregates: implications from spatial heterogeneity of organic carbon contents and carbon forms. *Biogeochemistry*, *85*(1), 45-57. https://doi.org/10.1007/s10533-007-9105-3

Li, J., Pei, J., Pendall, E., Reich, P. B., Noh, N. J., Li, B., … Nie, M. (2020). Rising temperature may trigger deep soil carbon loss across forest ecosystems. *Advanced Science*, 2001242. https://doi.org/10.1002/advs.202001242

Li, M., Han, X., Du, S., & Li, L. J. (2019). Profile stock of soil organic carbon and distribution in croplands of Northeast China. *Catena*, *174*, 285–292. https://doi.org/10.1016/j.catena.2018.11.027

Lian, Z., Jiang, Z., Huang, X., Liu, S., Zhang, J., & Wu, Y. (2018). Labile and recalcitrant sediment organic carbon pools in the Pearl River Estuary, southern China. *Science of the Total Environment*, *640*, 1302-1311. https://doi.org/10.1016/j.scitotenv.2018.05.389

Liao, C. Z., Luo, Y. Q., Fang, C. M., Chen, J. K., & Li, B. (2008). Litter pool sizes, decomposition, and nitrogen dynamics in *Spartina alterniflora*-invaded and native coastal marshlands of the Yangtze Estuary. *Oecologia*, *156*(3), 589-600. https://doi.org/10.1007/s0044 2-008-1007-0

Lin, T., Ye, S., Ma, C., Ding, X., Brix, H., Yuan, H., … Guo, Z. (2013). Sources and preservation of organic matter in soils of the wetlands in the Liaohe (Liao River) Delta, North China. *Marine Pollution Bulletin*, *71*(1-2), 276–285. https://doi.org/10.1016/j.marpolbul.2013.01.036

Liu, H., Ren, H., Hui, D., Wang, W., Liao, B., & Cao, Q. (2014). Carbon stocks and potential carbon storage in the mangrove forests of China. *Journal of Environmental Management*, *133*, 86–93. https://doi.org/10.1016/j.jenvman.2013.11.037

Lu, R. (2000). Analytical methods of soil agrochemistry. China Agricultural Science and Technology Press, Beijing, China.

Lu, W., Xiao, J., Liu, F., Zhang, Y., Liu, C., & Lin, G. (2017). Contrasting ecosystem CO_2 fluxes of inland and coastal wetlands: a meta-analysis of eddy covariance data. *Global Change Biology*, *23*(3), 1180–1198. https://doi.org/10.1111/gcb.13424

Luo, Z. K., & Raphael, V. R. (2020). Soil properties override climate controls on global soil organic carbon stocks. *Biogeosciences Discussion*, 1-24. https://doi.org/10.5194/bg-2020-298

Luo, Z., Feng, W., Luo, Y., Baldock, J., & Wang, E. (2017). Soil organic carbon dynamics jointly controlled by climate, carbon inputs, soil properties and soil carbon fractions. *Global Change Biology*, *23*(10), 4430–4439. https://doi.org/10.1111/gcb.13767

Ma, K., Liu, J., Zhang, Y., Parry, L. E., Holden, J., & Ciais, P. (2015). Refining soil organic carbon stock estimates for China's palustrine wetlands. *Environmental Research Letters*, *10*(12), 124016. https://doi.org/10.1088/1748-9326/10/12/124016

Melillo, J. M., Frey, S. D., DeAngelis, K. M., Werner, W. J., Bernard, M. J., Bowles, F. P., … Grandy, A. S. (2017). Long-term pattern and magnitude of soil carbon feedback to the climate system in a warming world. *Science*, *358*(6359), 101–105. https://doi.org/10.1126/science.aan2874

Meng, W., Feagin, R. A., Hu, B., He, M., & Li, H. (2019). The spatial distribution of blue carbon in the coastal wetlands of China. *Estuarine, Coastal and Shelf Science*, *222*, 13–20. https://doi.org/10.1016/j.ecss.2019.03.010

Meng, W., He, M., Hu, B., Mo, X., Li, H., Liu, B., & Wang, Z. (2017). Status of wetlands in China: A review of extent, degradation, issues and recommendations for improvement. *Ocean & Coastal Management*, *146*, 50–59. https://doi.org/10.1016/j.ocecoaman.2017.06.003

Mitsch, W. J., Bernal, B., Nahlik, A. M., Mander, Ü., Zhang, L., & Anderson, C. J., et al. (2013). Wetlands, carbon, and climate change. *Landscape Ecology, 28*(4), 583-597. https://doi.org/10.1007/s10980-012-9758-8

Moinet, G. Y. K., Hunt, J. E., Kirschbaum, M. U. F., Morcom, C. P., Midwood, A. J., & Millard, P. (2018). The temperature sensitivity of soil organic matter decomposition is constrained by microbial access to substrates. *Soil Biology and Biochemistry*, *116*, 333–339. https://doi.org/10.1016/j.soilbio.2017.10.031

Nahlik, A. M., & Fennessy, M. S. (2016). Carbon storage in us wetlands. *Nature Communications*, *7*, 13835. https://doi.org/10.1038/ncomms13835

O'Connor, J. J., Fest, B. J., Sievers, M., & Swearer, S. E. (2019). Impacts of land management practices on blue carbon stocks and greenhouse gas fluxes in coastal ecosystems – A meta-analysis. *Global Change Biology*, *26*, 1354–1366. https://doi.org/10.1111/gcb.14946

Olefeldt, D., & Roulet, N. T. (2012). Effects of permafrost and hydrology on the composition and transport of dissolved organic carbon in a subarctic peatland complex. *Journal of Geophysical Research*: *Biogeosciences*, *117*, G01005. https://doi.org/10.1029/2011jg001819

Osland, M. J., Gabler, C. A., Grace, J. B., Day, R. H., McCoy, M. L., McLeod, J. L., … Hartley, S. B. (2018). Climate and plant controls on soil organic matter in coastal wetlands. *Global Change Biology*, *24*, 5361–5379. https://doi.org/10.1111/gcb.14376

Pennock, D., Yates, T., Bedard-Haughn, A., Phipps, K., Farrell, R., & McDougal, R. (2010). Landscape controls on N_2O and CH_4 emissions from freshwater mineral soil wetlands of the Canadian Prairie Pothole region. *Geoderma*, *155*(3-4), 308–319. https://doi.org/10.1016/j.geoderma.2009.12.015

Poeplau, C., Kätterer, T., Leblans, N. I., & Sigurdsson, B. D. (2017). Sensitivity of soil carbon fractions and their specific stabilization mechanisms to extreme soil warming in a subarctic grassland. *Global Change Biology*, *23*(3), 1316-1327. https://doi.org/10.1111/gcb.13491

Prescott, C. E. (2010). Litter decomposition: What controls it and how can we alter it to sequester more carbon in forest soils? *Biogeochemistry*, *101*, 133–149. https://doi.org/10.1007/s10533-010-9439-0

Raich, J. W., & Tufekciogul, A. (2000). Vegetation and soil respiration: Correlations and controls. *Biogeochemistry*, *48*, 71–90. https://doi.org/10.1023/A:1006112000616

Rogers, K., Saintilan, N., & Woodroffe, C. D. (2014). Surface elevation change and vegetation distribution dynamics in a subtropical coastal wetland: Implications for coastal wetland response to climate change. *Estuarine*, *Coastal and Shelf Science*, *149*, 46–56. https://doi.org/10.1016/j.ecss.2014.07.009

Rovai, A. S., Twilley, R. R., Castañeda-Moya, E., Riul, P., Cifuentes-Jara, M., Manrow-Villalobos, M., … Pagliosa, P. R. (2018). Global controls on carbon storage in mangrove soils. *Nature Climate Change*, *8*(6), 534–538. https://doi.org/10.1038/s41558-018-0162-5

Rovira, P., & Ramón Vallejo, V. (2007). Labile, recalcitrant, and inert organic matter in Mediterranean forest soils. *Soil Biology and Biochemistry, 39(1)*, 202–215. https://doi.org/10.1016/j.soilbio.2006.07.021

Ru, N., Yang, X., Song, Z., Liu, H., Hao, Q., Liu, X., Wu, X. (2018). Phytoliths and phytolith carbon occlusion in aboveground vegetation of sandy grasslands in eastern Inner Mongolia. China. *Science of the Total Environment*, 625, 1283–1289. https://doi.org/10.1016/j.scitotenv.2018.01.055

Saintilan, N., Rogers, K., Mazumder, D., & Woodroffe, C. (2013). Allochthonous and autochthonous contributions to carbon accumulation and carbon store in southeastern Australian coastal wetlands. *Estuarine*, *Coastal and Shelf Science*, *128*, 84–92. https://doi.org/10.1016/j.ecss.2013.05.010

Sarker, T. C., Incerti, G., Spaccini, R., Piccolo, A., Mazzoleni, S., & Bonanomi, G. (2018). Linking organic matter chemistry with soil aggregate stability: Insight from ^{13}C NMR spectroscopy. *Soil Biology and Biochemistry*, *117*, 175-184. https://doi.org/10.1016/j.soilbio.2017.11.011

Schmidt, M. W., Torn, M. S., Abiven, S., Dittmar, T., Guggenberger, G., Janssens, I. A., ... & Trumbore, S. E. (2011). Persistence of soil organic matter as an ecosystem property. *Nature*, *478*(7367), 49-56. https://doi.org/10.1038/nature10386

Serrano, O., Lovelock, C. E., B. Atwood, T., Macreadie, P. I., Canto, R., Phinn, S., … Duarte, C. M. (2019). Australian vegetated coastal ecosystems as global hotspots for climate change mitigation. *Nature Communications*, *10*(1), 1–10. https://doi.org/10.1038/s41467-019-12176-8

State Forestry Administration. (2015). China wetlands resources. China: Forestry Publishing Press.

Sui, X., Zhang, R., Frey, B., Yang, L., Liu, Y., Ni, H., & Li, M. H. (2021). Soil physicochemical properties drive the variation in soil microbial communities along a forest successional series in a degraded wetland in northeastern China. *Ecology and Evolution*, *11*(5), 2194-2208. https://doi.org/10.1002/ece3.7184

Sun, H., Jiang, J., Cui, L., Feng, W., Wang, Y., & Zhang, J. (2019). Soil organic carbon stabilization mechanisms in a subtropical mangrove and salt marsh ecosystems. *Science of the Total Environment*, *673*, 502-510. https://doi.org/10.1016/j.scitotenv.2019.04.122

Sun, T., Wang, Y., Hui, D., Jing, X., & Feng, W. (2020). Soil properties rather than climate and ecosystem type control the vertical variations of soil organic carbon, microbial carbon, and microbial quotient. *Soil Biology and Biochemistry*, *148*, 107905. https://doi.org/10.1016/j.soilbio.2020.107905

Tangen, B. A., & Bansal, S. (2020). Soil organic carbon stocks and sequestration rates of inland, freshwater wetlands: Sources of variability and uncertainty. *Science of the Total Environment*, *749*, 141444. https://doi.org/10.1016/j.scitotenv.2020.141444

Throckmorton, H. M., Bird, J. A., Monte, N., Doane, T., Firestone, M. K., & Horwath, W. R. (2015). The soil matrix increases microbial C stabilization in temperate and tropical forest soils. *Biogeochemistry*, *122*(1), 35-45. https://doi.org/10.1007/s10533-014-0027-6

Vance, E. D., Brookes, P. C., & Jenkinson, D. S. (1987). An extraction method for measuring soil microbial biomass C. *Soil Biology and Biochemistry*, *19*(6), 703–707. https://doi.org/10.1016/0038-

0717(87)90052-6
Villa, J. A., & Bernal, B. (2018). Carbon sequestration in wetlands, from science to practice: An overview of the biogeochemical process, measurement methods, and policy framework. *Ecological Engineering*, *114*, 115–128. https://doi.org/10.1016/j.ecoleng.2017.06.037
Villa, J. A., & Mitsch, W. J. (2015). Carbon sequestration in different wetland plant communities in the Big Cypress Swamp region of southwest Florida. *International Journal of Biodiversity Science*, *Ecosystem Services & Management*, *11*(1), 17–28. https://doi.org/10.1080/21513732.2014.973909
Wang, G., Welham, C., Feng, C., Chen, L., & Cao, F. (2015). Enhanced soil carbon storage under agroforestry and afforestation in subtropical China. *Forests*, *6*(7), 2307-2323. https://doi.org/10.3390/f6072307
Wang, W., Sardans, J., Wang, C., Zeng, C., Tong, C., Chen, G., ... & Peñuelas, J. (2019). The response of stocks of C, N, and P to plant invasion in the coastal wetlands of China. *Global Change Biology*, *25*(2), 733-743. https://doi.org/10.1111/gcb.14491
Wang, Z., He, Y., Niu, B., Wu, J., Zhang, X., Zu, J., … Wang, X. (2020). Sensitivity of terrestrial carbon cycle to changes in precipitation regimes. *Ecological Indicators*, *113*, 106223. https://doi.org/10.1016/j.ecolind.2020.106223
Whitaker, K., Rogers, K., Saintilan, N., Mazumder, D., Wen, L., & Morrison, R. J. (2015). Vegetation persistence and carbon storage: implications for environmental water management for *Phragmites australis*. *Water Resources Research*, *51*, 5284–5300. https://doi.org/10.1002/2014WR016253
Xia, S., Song, Z., Li, Q., Guo, L., Yu, C., Pal Singh, B., … Wang, H. (2021a). Distribution, sources, and decomposition of soil organic matter along a salinity gradient in estuarine wetlands characterized by C:N ratio, $\delta^{13}C$-$\delta^{15}N$ and lignin biomarker. *Global Change Biology*, *27*, 417-434. https://doi.org/10.1111/gcb.15403
Xia, S., Wang, W., Song, Z., Yakov K., Guo, L., Lukas, V. Z., …Wang, H. (2021b). *Spartina alterniflora* invasion controls organic carbon stocks in coastal marsh and mangrove soils across tropics and subtropics. *Global Change Biology*, *27*, 1627-1644. https://doi.org/10.1111/gcb.15516
Xiao, D., Deng, L., Dong-Gill, Kim, Huang, C., & Tian, K. (2019). Carbon budgets of wetland ecosystems in China. *Global Change Biology*, 25, 2061–2076. https://doi.org/10.1111/gcb.14621
Xiong, Y., Liao, B., Proffitt, E., Guan, W., Sun, Y., Wang, F., & Liu, X. (2018). Soil carbon storage in mangroves is primarily controlled by soil properties: A study at Dongzhai Bay, China. *Science of the Total Environment*, *619*, 1226-1235. https://doi.org/10.1016/j.scitotenv.2017.11.187
Xu, L., Yu, G., He, N., Wang, Q., Gao, Y., Wen, D., … Ge, J. (2018). Carbon storage in China's terrestrial ecosystems: A synthesis. *Scientific Reports*, *8*(1), 2806. https://doi.org/10.1038/s41598-018-20764-9
Yan, Y., Zhao, B., Chen, J., Guo, H., Gu, Y., Wu, Q., & Li, B. (2008). Closing the carbon budget of estuarine wetlands with tower-based measurements and MODIS time series. *Global Change Biology*, *14*(10), 2469–2471. https://doi.org/10.1111/j.1365-2486.2008.01692.x
Yang, R. (2019). Interacting effects of plant invasion, climate, and soils on soil organic carbon storage in coastal wetlands. *Journal of Geophysical Research: Biogeosciences*, *12*(8), 2254-2264. https://doi.org/10.1029/2019jg005190
Yang, W., An, S., Zhao, H., Xu, L., Qiao, Y., & Cheng, X. (2016). Impacts of *Spartina alterniflora* invasion on soil organic carbon and nitrogen pools sizes, stability, and turnover in a coastal salt marsh of eastern China. *Ecological Engineering*, *86*, 174-182. https://doi.org/10.1016/j.ecoleng.2015.11.010
Yang, Y., Mohammat, A., Feng, J., Zhou, R., & Fang, J. (2007). Storage, patterns and environmental controls of soil organic carbon in China. *Biogeochemistry*, *84*(2), 131–141. https://doi.org/10.1007/s10533-007-9109-z

Yu, C., Xie, S., Song, Z., Xia, S., & Åström, M. E. (2021). Biogeochemical cycling of iron (hydr-)oxides and its impact on organic carbon turnover in coastal wetlands: A global synthesis and perspective. *Earth-Science Reviews*, *218*, 103658. https://doi.org/10.1016/j.earscirev.2021.10365

Zhang, Y., Li, C., Trettin, C. C., Li, H., & Sun, G. (2002). An integrated model of soil, hydrology, and vegetation for carbon dynamics in wetland ecosystems. *Global Biogeochemical Cycles*, *16*(4), 9-1-9-17. https://doi.org/10.1029/2001GB001838

Zheng, Y. M., Niu, Z. G., Gong, P., Dai, Y. J., & Shangguan, W. (2013). Preliminary estimation of the organic carbon pool in China's wetlands. *Chinese Science Bulletin*, *58*, 662–670. https://doi.org/10.1007/s11434-012-5529-9

Zhou, X., Xu, X., Zhou, G., & Luo, Y. (2018). Temperature sensitivity of soil organic carbon decomposition increased with mean carbon residence time: Field incubation and data assimilation. *Global Change Biology*, *24*(2), 810–822. https://doi.org/10.1111/gcb.13994

Figure Captions

FIGURE 1 Distributions of sampling locations along the temperate-subtropical-tropical climate zone in China's coastal wetlands, including 108 sampling sites from Liaoning Province (the north) to Hainan Province (the far south). Circles represent sites with our concurrent field and lab measurements, triangles denote sites or samples compiled with data from literature, and diamonds represent those with data extrapolated from similar wetlands.

FIGURE 2 Relationships between soil organic carbon (SOC) content and bulk density (BD) in China's coastal wetlands. Data presented here included 412 paired SOC content and bulk density measurements for different layers in filed samples, including 0–100 cm layer in LRD, DLJR, NDG and YRE, and 0–40 cm layer in CI, HI, YB, MRE, JRE, ZRE, ZJ and BH. The formula was modeled from the paired data points of all samples in the light blue region. The formulas of different colors were modeled from the paired data points of different soil layers. A logarithmic line model is used to estimate the bulk density for soils without the measured data.

FIGURE 3 Vertical distributions of SOC contents (mean ± SD) in the top 0–40 cm profile based on sampling location (A), vegetation type (B), invasion type (C; *P. australis* invaded by *S. alterniflora*, *K. obovate* invaded by *S. alterniflora*, *A. marina* invaded by *S. alterniflora*) and climatic zone (D).

FIGURE 4 Vertical distributions of SOC density (mean ± SD) in the 0–100 cm profile based on sampling location (A), vegetation type (B), invasion type with invasive species *S. alterniflora* (C) and climatic zone (D). All the data analyzed were collected from our field survey and lab measurements.

FIGURE 5 Pearson correlations between soil parameters and SOC content in independent wetlands (A), climate zones (B), vegetation types (C), and invasion types (D). Abbreviations: SOC, soil organic carbon; TN, total nitrogen; MBC, microbial biomass carbon; DOC, dissolved organic carbon; TP, total phosphorus; EC, electrical conductance; SWC, soil water content; BD, bulk density; S/V, the syringyl-to-vanillyl ratio; C/V, the cinnamyl-to-vanillyl ratio; (Ad/Al)v, the acid-to-aldehyde ratio of vanillyl unit; (Ad/Al)s, the acid-to-aldehyde ratio of syringyl unit; Λ_8, organic carbon (OC)-normalized concentration of lignin phenols (V+S+C).

FIGURE 6 Relationships between MAT (°C) and SOC density in the 0–40 cm (A) and 40–100 cm (B) profiles, and between MAP (mm) and SOC density in the 0–40 cm (C) and 40–100 cm (D) profiles.

FIGURE 7 Variance partitioning analysis (VPA) for SOC contents in China's coastal wetlands. Soil chemical properties here include MBC, DOC, TN, TP, pH, and EC; Soil physical properties include SWC, BD, and particle size composition (clay, silt and sand); Climate include MAT and MAP. The numbers in the circles indicate the explained values, residuals represent unexplained value.

FIGURE 8 The relative importance of predictor variables from the regression prediction analysis using random forest of the changes to SOC content (A) and density (B). The relative influence of three categories of variables are calculated as the sum of the relative importance of individual variables in each variable group (i.e., soil chemical properties, soil physical properties, and lignin reflecting litter input and composition). Soil chemical properties here include DOC, TP, pH, EC and MBC; Soil physical properties include BD, SWC, clay, silt and sand; and plant traits include lignin content Λ_8, S/V, C/V, (Ad/Al)v, and (Ad/Al)s. Red columns indicate that variables have significant differences ($p < 0.05$) in SOC contents.

FIGURE 9 Vegetation composition and distributions in terms of tidal actions, and aboveground biomass with SOC density depending on each vegetation type. Green histograms represent the relative size of aboveground biomass of a given vegetation. Blue histograms represent the relative size of SOC density vegetated corresponding plants in the top 0–40 cm, and pink histograms are SOC densities in the 40–100 cm layer.

FIGURE 10 Schematic showing the distributions of SOC density among different wetland types in the critical wetland zone. There are four wetland types (i.e., lake, river, coastal, and marsh) integrated with our field measurements and regional characteristics. The SOC density in top 1 m of lake, river and marsh wetlands are derived from Xiao et al. (2019).

Figure 1

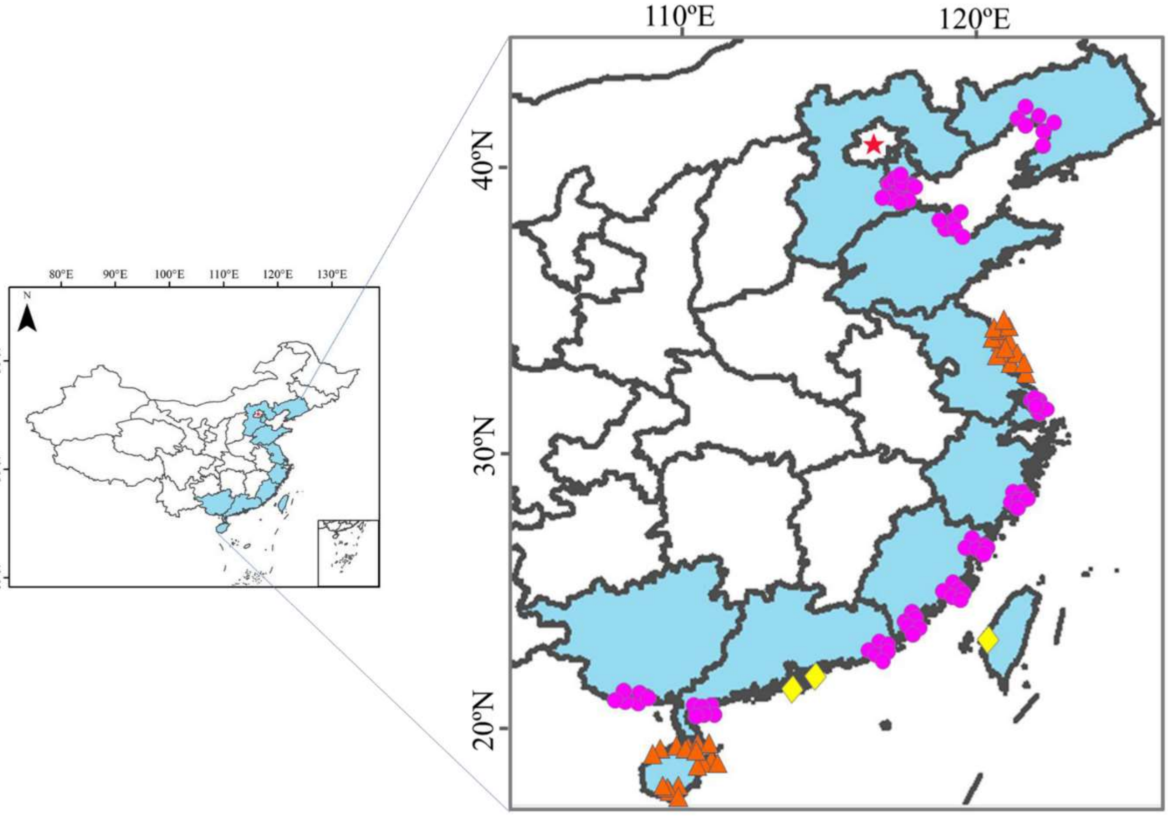

80°E
90°E
100°E
110°E
120°E
130°E
N
50°N
30°N
10°N
110ºE
120ºE
40ºN
30ºN
20ºN

Figure 2

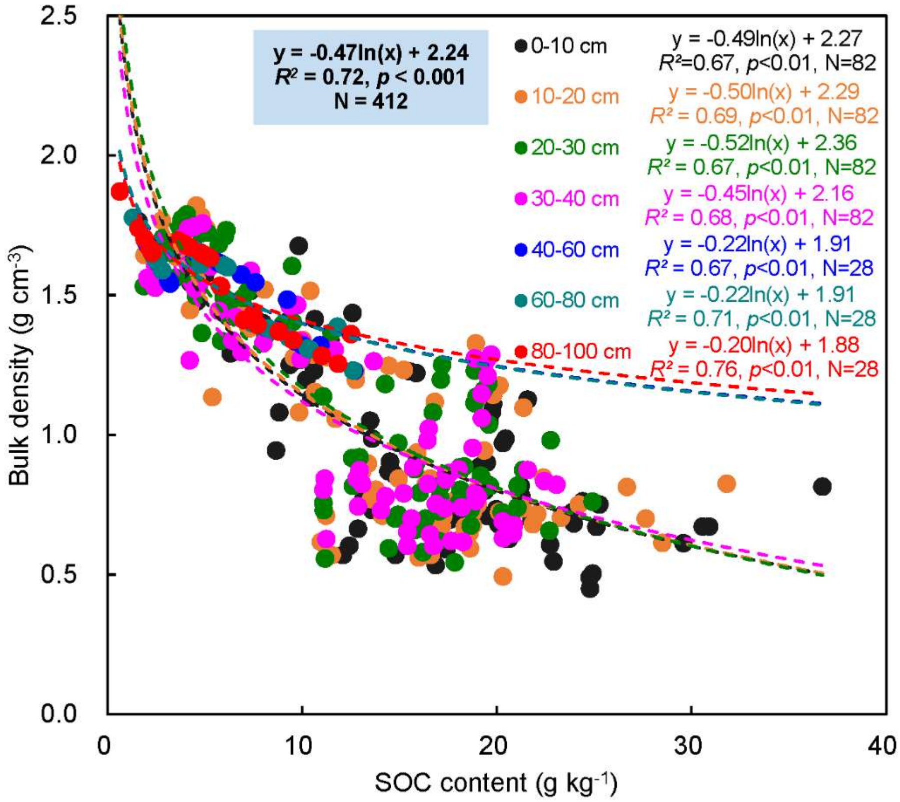
y = -0.47ln(x) + 2.24
R² = 0.72, p < 0.001
N = 412
0-10 cm
y = -0.49ln(x) + 2.27
R²=0.67, p<0.01, N=82
10-20 cm
y = -0.50ln(x) + 2.29
R² = 0.69, p<0.01, N=82
20-30 cm
y = -0.52ln(x) + 2.36
R² = 0.67, p<0.01, N=82
30-40 cm
y = -0.45ln(x) + 2.16
R² = 0.68, p<0.01, N=82
40-60 cm
y = -0.22ln(x) + 1.91
R² = 0.67, p<0.01, N=28
60-80 cm
y = -0.22ln(x) + 1.91
R² = 0.71, p<0.01, N=28
80-100 cm
y = -0.20ln(x) + 1.88
R² = 0.76, p<0.01, N=28
Bulk density (g cm-3)
SOC content (g kg-1)
2.5
2.0
1.5
1.0
0.5
0.0
0
10
20
30
40

Figure 3

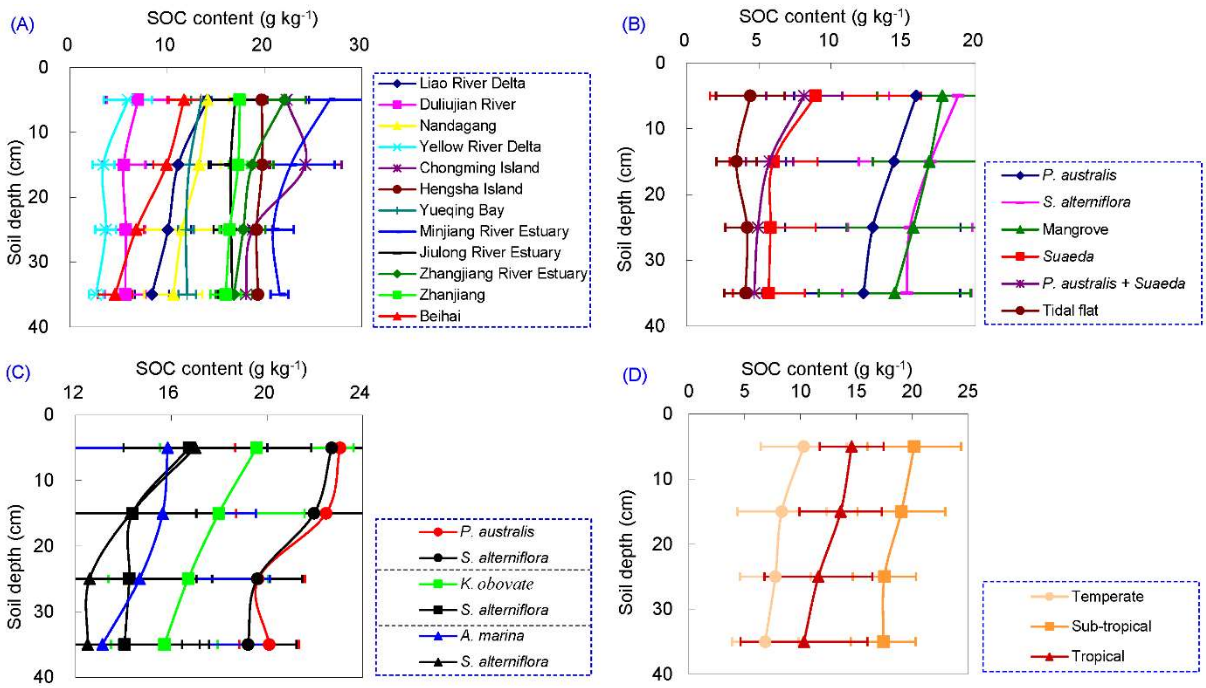
(A)
SOC content (g kg-1)
0
10
20
30
Soil depth (cm)
Liao River Delta
Duliujian River
Nandagang
Yellow River Delta
Chongming Island
Hengsha Island
Yueqing Bay
Minjiang River Estuary
Jiulong River Estuary
Zhangjiang River Estuary
Zhanjiang
Beihai
(B)
SOC content (g kg-1)
0
5
10
15
20
Soil depth (cm)
P. australis
S. alterniflora
Mangrove
Suaeda
P. australis + Suaeda
Tidal flat
(C)
SOC content (g kg-1)
12
16
20
24
Soil depth (cm)
P. australis
S. alterniflora
K. obovate
S. alterniflora
A. marina
S. alterniflora
(D)
SOC content (g kg-1)
0
5
10
15
20
25
Soil depth (cm)
Temperate
Sub-tropical
Tropical

Figure 4

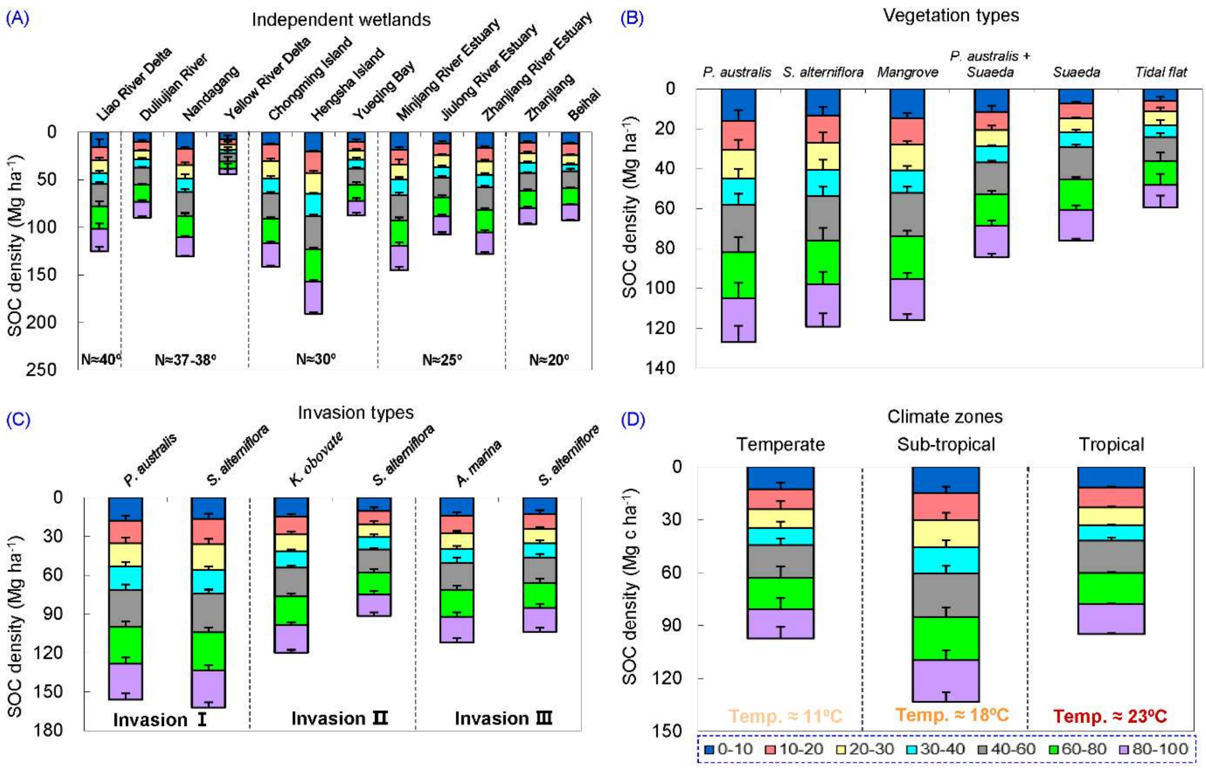

(A)
Independent wetlands
Liao River Delta
Duliujian River
Nandagang
Yellow River Delta
Chongming Island
Hengsha Island
Yueqing Bay
Minjiang River Estuary
Jiulong River Estuary
Zhanjiang River Estuary
Zhanjiang
Beihai
SOC density (Mg ha-1)
0
50
100
150
200
250
N≈40°
N≈37-38°
N≈30°
N≈25°
N≈20°
(B)
Vegetation types
P. australis
S. alterniflora
Mangrove
P. australis + Suaeda
Suaeda
Tidal flat
SOC density (Mg ha-1)
0
20
40
60
80
100
120
140
(C)
Invasion types
P. australis
S. alterniflora
K. obovate
S. alterniflora
A. marina
S. alterniflore
SOC density (Mg ha-1)
0
30
60
90
120
150
180
Invasion Ⅰ
Invasion Ⅱ
Invasion Ⅲ
(D)
Climate zones
Temperate
Sub-tropical
Tropical
SOC density (Mg c ha-1)
0
30
60
90
120
150
Temp. ≈ 11°C
Temp. ≈ 18°C
Temp. ≈ 23°C
0-10
10-20
20-30
30-40
40-60
60-80
80-100

Figure 5

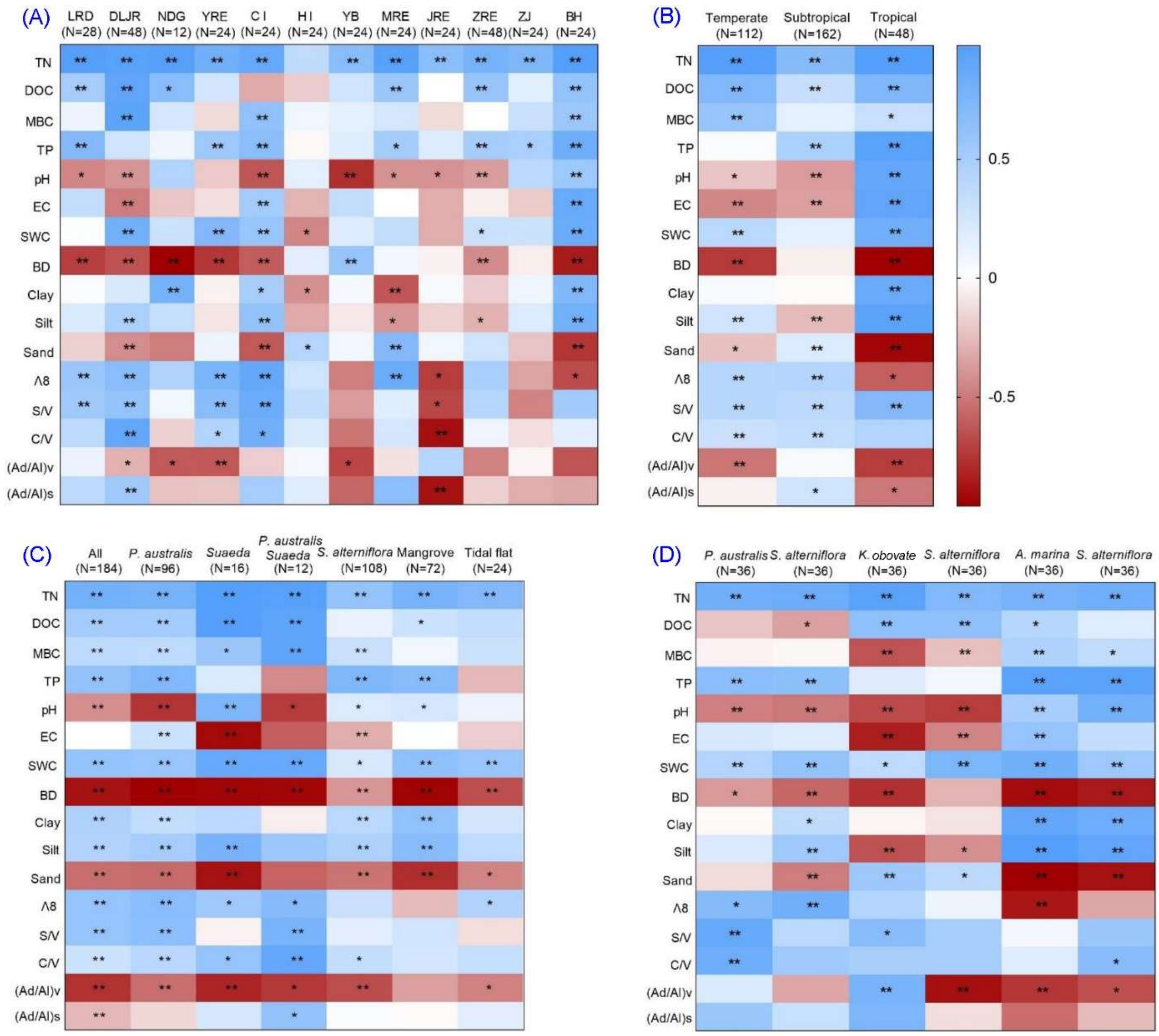
(A)
LRD (N=28)
DLJR (N=48)
NDG (N=12)
YRE (N=24)
C I (N=24)
H I (N=24)
YB (N=24)
MRE (N=24)
JRE (N=24)
ZRE (N=48)
ZJ (N=24)
BH (N=24)
(B)
Temperate (N=112)
Subtropical (N=162)
Tropical (N=48)
(C)
All (N=184)
P. australis (N=96)
Suaeda (N=16)
P. australis Suaeda (N=12)
S. alterniflora (N=108)
Mangrove (N=72)
Tidal flat (N=24)
(D)
P. australis (N=36)
S. alterniflora (N=36)
K. obovate (N=36)
S. alterniflora (N=36)
A. marina (N=36)
S. alterniflora (N=36)
TN
DOC
MBC
TP
pH
EC
SWC
BD
Clay
Silt
Sand
Λ8
S/V
C/V
(Ad/Al)v
(Ad/Al)s
0.5
0
-0.5

Figure 6

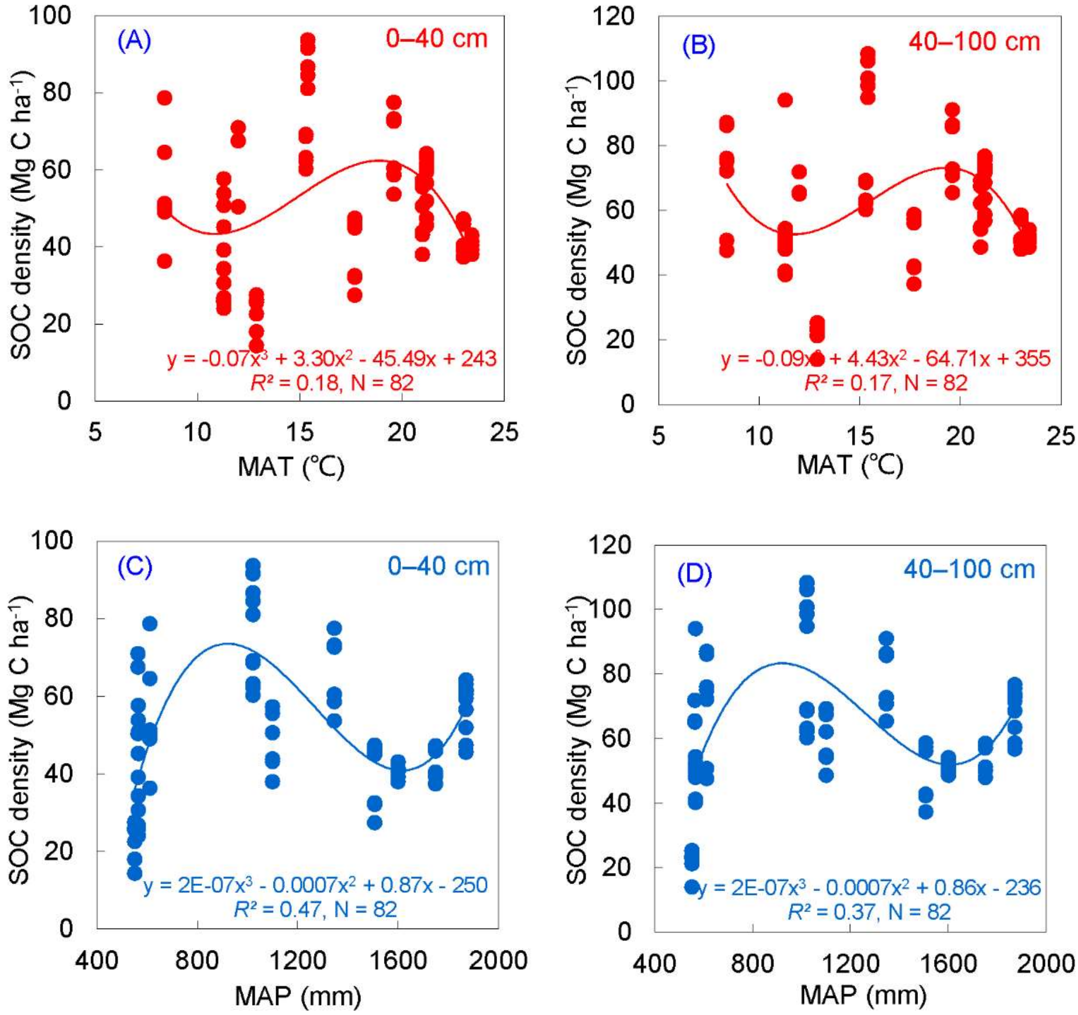
(A)
0–40 cm
y = -0.07x³ + 3.30x² - 45.49x + 243
R² = 0.18, N = 82
SOC density (Mg C ha⁻¹)
MAT (℃)
(B)
40–100 cm
y = -0.09x³ + 4.43x² - 64.71x + 355
R² = 0.17, N = 82
SOC density (Mg C ha⁻¹)
MAT (℃)
(C)
0–40 cm
y = 2E-07x³ - 0.0007x² + 0.87x - 250
R² = 0.47, N = 82
SOC density (Mg C ha⁻¹)
MAP (mm)
(D)
40–100 cm
y = 2E-07x³ - 0.0007x² + 0.86x - 236
R² = 0.37, N = 82
SOC density (Mg C ha⁻¹)
MAP (mm)

Figure 7

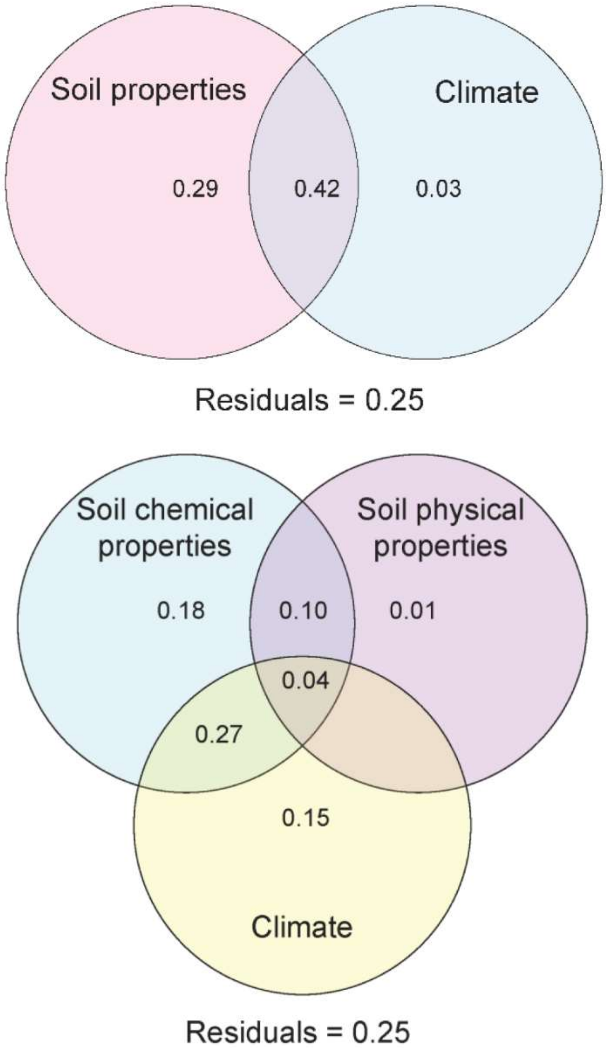
Soil properties
Climate
0.29
0.42
0.03
Residuals = 0.25
Soil chemical properties
Soil physical properties
0.18
0.10
0.01
0.04
0.27
0.15
Climate
Residuals = 0.25

Figure 8

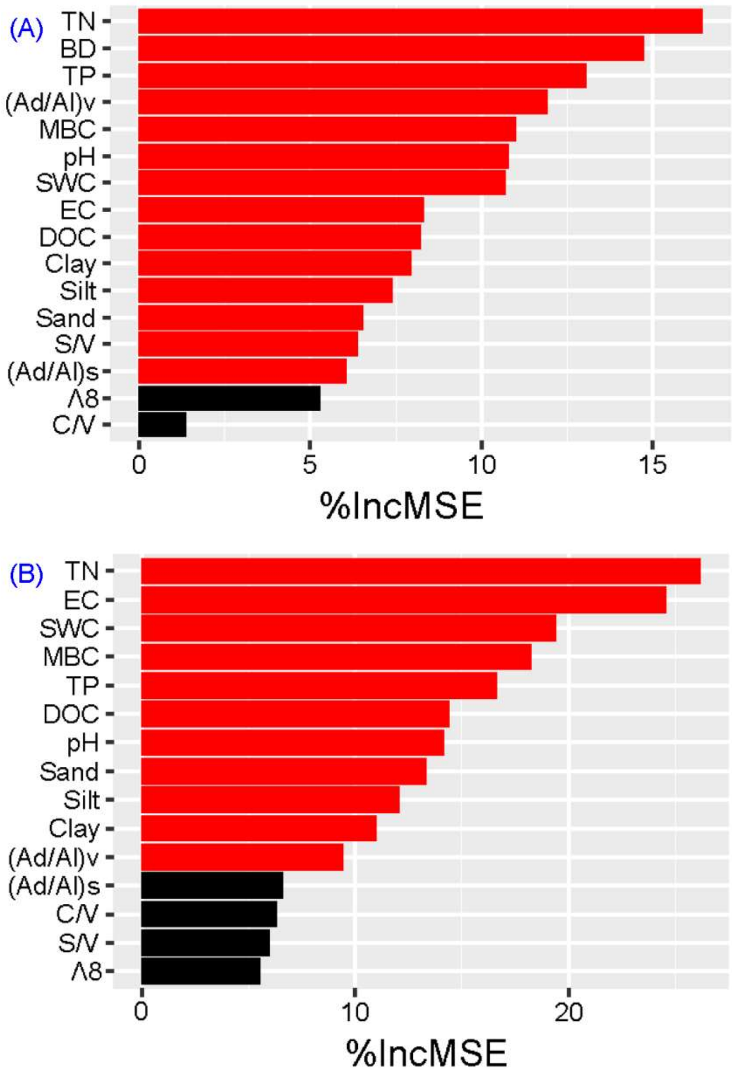
(A)
TN
BD
TP
(Ad/Al)v
MBC
pH
SWC
EC
DOC
Clay
Silt
Sand
S/V
(Ad/Al)s
Λ8
C/V
0
5
10
15
%IncMSE
(B)
TN
EC
SWC
MBC
TP
DOC
pH
Sand
Silt
Clay
(Ad/Al)v
(Ad/Al)s
C/V
S/V
Λ8
0
10
20
%IncMSE

Figure 9

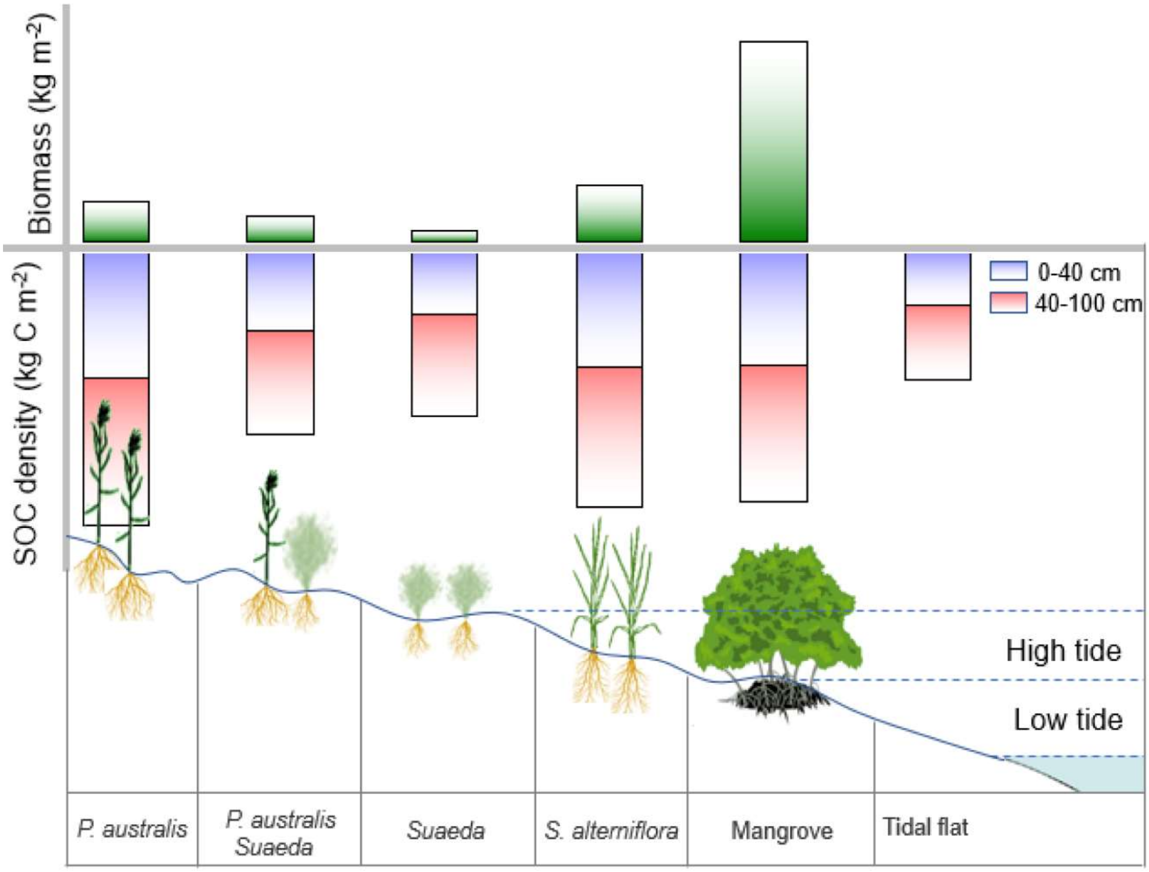

Biomass (kg m^{-2})
SOC density (kg C m^{-2})
0-40 cm
40-100 cm
High tide
Low tide
P. australis
P. australis
Suaeda
Suaeda
S. alterniflora
Mangrove
Tidal flat

Figure 10

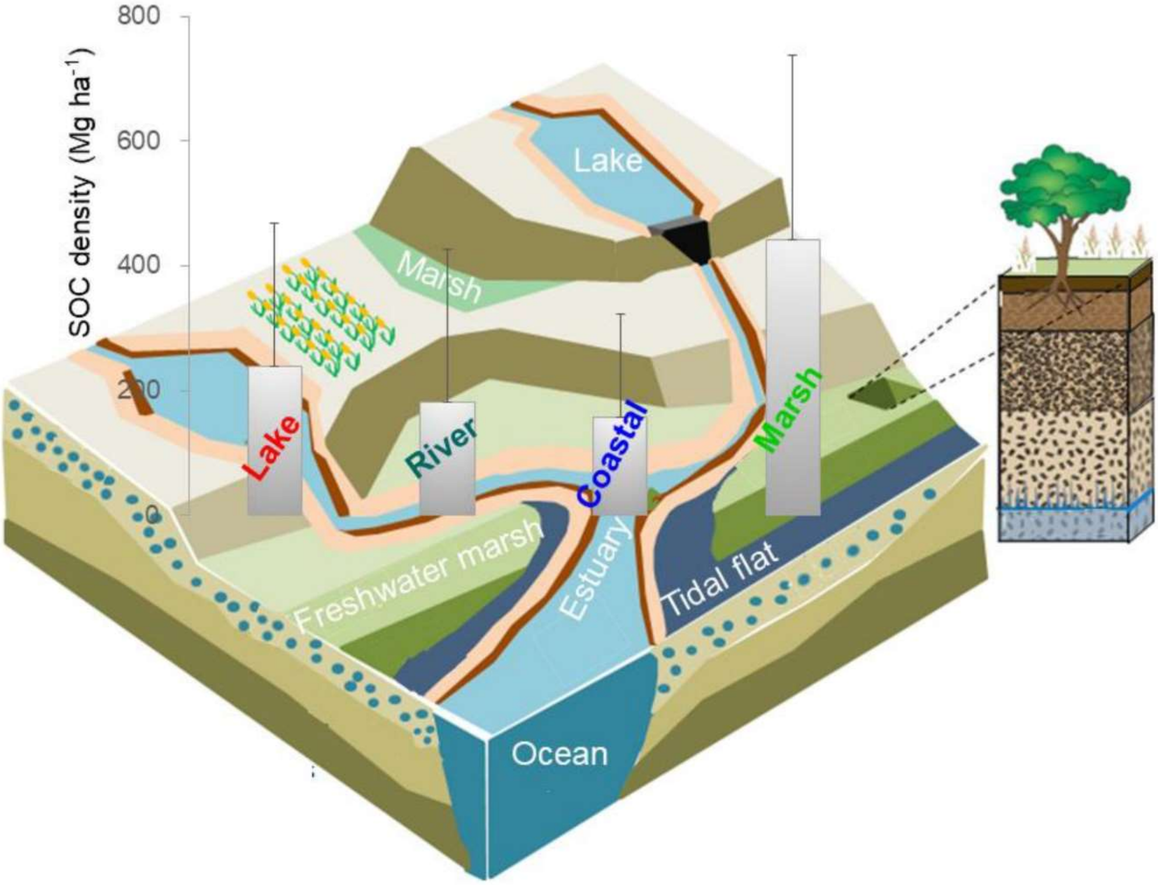

800
600
400
200
0
SOC density (Mg ha-1)
Lake
Marsh
Lake
River
Coastal
Marsh
Freshwater marsh
Estuary
Tidal flat
Ocean

Table 1 Summary of SOC sequestration capacity in coastal wetlands of China synthesized from sampled soil cores and literature data

Province/ city	Area of coastal wetlands (10^3 ha) [a]	Soil depth (cm)	SOC stock (Mg ha^{-1})	Representative wetlands	SOC sequestration (10^6 Mg)	Main plants	The number of samples (sites × layers)	References
Liaoning	97.47	0–40	54.34±12.51	Liao River Delta (LRD)	5.30±1.22	*P. australis*, *S. glauca*, *S. salsa*, Tidal flat	49 (7 × 7)	This study
		40–100	70.77±14.59		6.90±1.42			
Tianjin	18.97	0–40	37.45±11.33	Duliujian River (DLJR)	0.71±0.21	*P. australis*, *S. glauca*, *S. salsa*, Tidal flat	84 (12 × 7)	This study
		40–100	52.40±13.21		0.99±0.25			
Hebei	18.65	0–40	63.01±9.00	Nandagang wetland (NDG)	1.18±0.17	*P. australis*, *S. glauca*, *S. salsa*, Tidal flat	21 (3 × 7)	This study
		40–100	67.58±3.11		1.26±0.06			
Shandong	76.34	0–40	22.43±4.74	Yellow River Estuary (YRE)	1.71±0.36	*P. australis*, *S. glauca*, *S. salsa*, *S. alterniflora*, Tidal flat	42 (6 × 7)	This study
		40–100	21.77±3.67		1.66±0.28			
Jiangsu	52.88	0–100	47.61±21.97	Wanggang Wetland (WGW), Yancheng Wetland (YCW), Dafeng Wetland (DW)	2.52±1.16	*P. australis*, *S. salsa*, *S. alterniflora*, *A. littoralis*	22 sites	Gao et al., 2016; Liu et al., 2017; Zang, 2019; Yang, 2019; Yang et al., 2016; Fu et al., 2021
Shanghai	71.25	0–40	76.40±12.50	Chongming Island (CI), Hengsha Island (HI)	5.44±0.89	*P. australis*, *S. alterniflora*	84 (12 × 7)	This study
		40–100	89.85±13.43		6.40±0.96			
Zhejiang	29.51	0–40	38.49±7.93	Yueqing Bay (YB)	1.14±0.23	*K. obovate*, *S. alterniflora*	42 (6 × 7)	This study
		40–100	49.16±8.51		1.45±0.25			
Fujian	34.23	0–40	57.51±9.46	Minjiang River Estuary (MRE), Jiulong River Estuary (JRE), Zhangjiang River Estuary (ZRE)	1.97±0.32	*P. australis*, *S. alterniflora*, *K. obovate*, *A. marina*,	168 (24 × 7)	This study
		40–100	69.57±10.16		2.38±0.35			
Guangdong	49.37	0–40	42.94±3.95	Zhanjiang (ZJ)	2.12±0.20	*A. marina*, *S. alterniflora*	42 (6 × 7)	This study
		40–100	53.94±4.24		2.66±0.21			
Guangxi	81.88	0–40	40.91±1.86	Beihai (BH)	3.35±0.15	*A. marina*,	42	This study

		40–100	51.76±2.00		4.24±0.16	*S. alterniflora*	(6 × 7)	
Hainan	10.23	0–100	315.21±248.58	Dongzhai Bay (DB), Qinglan Harbor (QH), Xinying Harbor (XB), Sanya Bay (SYB), Sibi Bay (SBB), Xinyang Bay (XB), Tielu Harbor (TH), Danzhou (DZ), Lingao (LG)	3.22±2.54	*S. apetala*, *K. obovate*, *R. stylosa*, *A. marina*, *A. corniculatum*, *B. sexangular*, *C. tagal*, *B. gymnorrhiza*	38 sites	Gao et al., 2019; Wang et al., 2019; Huang et al., 2017; Xiong et al., 2018; Xin et al., 2014; Lin et al., 2015; Gao et al., 2018; Fu et al., 2021
Hong Kong[b]	0.11	0–100	110.90±5.30 ~ 160.3±21.00	—	0.09±0.01	—	—	Fu et al., 2021
Macao[b]	0.01	0–100	110.90±5.30 ~ 160.30±21.00	—	0.00±0.00	—	—	Fu et al., 2021
Taiwan[c]	20.35	0–100	135.80±25.90 ~ 192.00±23.80	—	0.13±0.02	—	—	Fu et al., 2021

[a]The data of area of coastal wetlands in each Province of China along coastlines was originated from Mao et al. (2020);

[b]SOC stocks Hong Kong and Macao was substituted by the data of Pearl River Estuary;

[c]SOC stocks in Taiwan was substituted by the data of Fujian, Guangdong, Guangxi and Hainan.

Table 2 Stepwise multiple regression analysis between SOC contents and environmental factors

Classification basis		Regression equation	R^2	*p* value	Std. error of the estimate	*N*	Extracted parameters
Vegetation types	*P. australis*	Y=-21.53+7.85TN+0.02MAP+0.01MBC-0.02DOC-0.15SWC+7.34TP+1.41pH-4.53$(Ad/Al)_V$	0.98	<0.001	1.31	96	TN, MAP, MBC, DOC, SWC, TP, pH, $(Ad/Al)_V$
	Suaeda	Y=0.07+7.97TN	0.98	<0.001	0.62	16	TN
	P. australis, *Suaeda*	Y=-2.39+11.86TN	0.92	<0.001	0.61	12	TN
	S. alterniflora	Y=30.20-47.59$(Ad/Al)_V$+11.13TN-0.68MAT-0.11Λ_8-0.001EC+0.02DOC	0.91	<0.001	1.64	108	$(Ad/Al)_V$, TN, MAT, Λ_8, EC, DOC
	Mangrove	Y=24.55-15.22BD-0.001EC+0.02DOC+0.20SWC	0.96	<0.001	1.08	72	BD, EC, DOC, SWC
	Tidal flat	Y=7.79+7.43TN+0.10Clay-0.70MAT-0.02DOC	0.83	<0.001	0.81	24	TN, Clay, MAT, DOC
Invasion types	*P. australis*	Y=19.75+6.97TN-0.22SWC	0.91	<0.001	1.26	36	TN, SWC
	S. alterniflora	Y=-14.68+11.41TN+1.69pH+0.21Sand+0.02DOC	0.98	<0.001	0.73	36	TN, pH, Sand, DOC
	K. obovate	Y=2.97+9.07TN+3.52C/V	0.98	<0.001	0.61	36	TN, C/V
	S. alterniflora	Y=49.14-150.56$(Ad/Al)_V$+27.25$(Ad/Al)_S$	0.89	<0.001	1.32	36	$(Ad/Al)_V$, $(Ad/Al)_S$
	A. marina	Y=52.35+0.24SWC-2.21MAT+4.02TP+0.37pH-2.87BD	0.99	<0.001	0.23	36	SWC, MAT, TP, pH, BD
	S. alterniflora	Y=14.75-7.17BD+9.78TP	0.95	<0.001	1.15	36	BD, TP
Climate zone	Temperate	Y=4.88+8.17TN+0.004MBC-0.07SWC-2.35BD	0.95	<0.001	1.11	112	TN, BD, MBC, SWC, BD
	Subtropical	Y=5.57+8.78TN+5.70BD+0.005MBC+0.03DOC-0.001EC-22.18$(Ad/Al)_V$	0.90	<0.001	1.47	168	TN, BD, MBC, DOC, EC, $(Ad/Al)_V$
	Tropical	Y=3.71+4.23TN-4.03BD+0.07SWC+0.64pH	0.99	<0.001	0.41	48	TN, BD, SWC, pH